A STUDY OF PRECODING SCHEMES FOR OFDM SYSTEMS

THESIS SUBMITTED TO

THE GRADUATE SCHOOL OF NATURAL AND APPLIED SCIENCES
OF
MIDDLE EAST TECHNICAL UNIVERSITY

BY

F. SELCEN ÇAKAR

IN PARTIAL FULFILLMENT OF THE REQUIREMENTS
FOR
THE DEGREE OF MASTER OF SCIENCE
IN
ELECTRICAL AND ELECTRONICS ENGINEERING

AUGUST 2008

Approval of the thesis:

A STUDY OF PRECODING SCHEMES FOR OFDM SYSTEMS

submitted by **F. SELCEN ÇAKAR** in partial fulfillment of the requirements for the degree of **Master of Science in Electrical and Electronics Engineering Department, Middle East Technical University** by,

Prof. Dr. Canan Özgen ______________
Dean, Graduate School of **Natural and Applied Sciences**

Prof. Dr. İsmet Erkmen ______________
Head of Department, **Electrical and Electronics Engineering**

Assist. Prof. Dr. Çağatay Candan ______________
Supervisor, **Electrical and Electronics Engineering Dept., METU**

Assist. Prof. Dr. Ali Özgür Yılmaz ______________
Co-Supervisor, **Electrical and Electronics Engineering Dept., METU**

Examining Committee Members:

Prof. Dr. Engin Tuncer ______________
Electrical and Electronics Engineering Dept., METU

Assist. Prof. Dr. Çağatay Candan ______________
Electrical and Electronics Engineering Dept., METU

Assoc. Prof. Dr. Tolga Çiloğlu ______________
Electrical and Electronics Engineering Dept., METU

Assoc. Prof. Dr. Ali Özgür Yılmaz ______________
Electrical and Electronics Engineering Dept., METU

Dr.Alper Kutay ______________
TUBITAK, ILTAREN

Date: 25/08/2008

I hereby declare that all information in this document has been obtained and presented in accordance with academic rules and ethical conduct. I also declare that, as required by these rules and conduct, I have fully cited and referenced all material and results that are not original to this work.

Name, Last name: Selcen Çakar

Signature :

ABSTRACT

A STUDY OF PRECODING SCHEMES FOR OFDM SYSTEMS

Çakar, F. Selcen

M.S., Department of Electrical and Electronics Engineering
Supervisor: Assist. Prof. Dr. Çağatay Candan
Co-Supervisor: Assist. Prof. Dr. Ali Özgür Yılmaz

August 2008, 71 pages

We examine the effect of precoding on OFDM systems. The precoding operation, which is also known as constellation rotation, leads to a gain in diversity order for fading channels.

In this thesis, we examine the effect of precoding for different receivers such as Maximum Likelihood (ML), Minimum Mean Squared Error (MMSE), and Zero Forcing (ZF) receivers. The diversity gain due to precoding comes at no cost of bandwidth expansion or power increase. Therefore it is an attractive and practical alternative. We also examine the precoding gain, when some reduction of rate is tolerable and compare the performance of rate reduced system with the uncoded system with the system which is coded by rateless unitary precoders, and with the hard-decision decoded BCH coded coded system.

Keywords: Diversity, Rotational codes, Precoding, Fading Channels, OFDM, precoded OFDM

ÖZ

OFDM SİSTEMLERİ İÇİN ÖNKODLAMA YÖNTEMLERİ
İLE İLGİLİ BİR ÇALIŞMA

Çakar, F. Selcen

Yüksek Lisans, Elektrik ve Elektronik Mühendisliği Bölümü
Tez Yöneticisi: Y.Doç.Dr. Çağatay Candan
Ortak Tez Yöneticisi Y. Doç. Dr. Ali. Özgür Yılmaz

Ağustos 2008, 71 sayfa

Önkodlamanın OFDM sistemler üzerindeki etkisi incelenmiştir. Yıldızkümesi dönüşümü olaral da bilinen önkodlama işlemi sönümlü kanallar üzerinde bir çeşitleme kazancına yol açmaktadır.

Bu tezde, ML, MMSE ve ZF alıcıları gibi farklı alıcılar için önkodlamanın etkisini araştırdık. Önkodlamadan kaynaklanan çeşitleme kazancı herhangi bir güç kaybı ve band genişliği arttırımı olmadan gelmektedir. Bu nedenle ilginç ve pratik bir alternatif olarak karşımıza çıkmaktadır. Buna ek olarak, önkodlama kazancı hızın azalmasının tolere edilebileceği durumlar için incelenmiştir. Hızı düşürülmüş önkodlamalı sistem performansı önkodlamasız sistem performansı ve sıfır-bir karar dekodlamalı BCH kod sitem performansı ile karşılaştırılmıştır.

Anahtar Kelimeler: Çeşitleme, Dönüşümsel Kodlar, Ön Kodlama, Sönümlü Kanallar, OFDM, Ön-kodlamalı OFDM

ACKNOWLEDGEMENTS

First, I would like to express my gratitude to my supervisor, Cagatay Candan, for his guidance and invaluable advice, for sharing his insight and for reviewing the manuscript. Without his technical insight and continuous guidance I would never have been able to complete this thesis. I would also like to thank my co-advisor, Ali Özgür Yılmaz, for his invaluable help and reviews.

I want to thank TÜBİTAK for the financial support they provided for two years of my study.

I express my sincere thanks to my husband, Murat Sahin, for his endless support and love, for his tolerance and for making my life easier in this process.

Finally I must thank my family for their endless support and love during my whole life.

TABLE OF CONTENTS

LIST OF FIGURES

FIGURES

LIST OF ABBREVATIONS

AWGN	: Additive White Gaussian Noise
BER	: Bit Error Rate
BCH	: Bose–Chaudhuri–Hocquenghem
BPSK	: Binary Phase Shift Keying
CP	: Cyclic Prefix
CR	: Cyclic Removal
DFT	: Discrete Fourier Transform
FFT	: Fast Fourier Transform
IBI	: Inter Block Interference
IDFT	: Inverse Discrete Fourier Transform
IFFT	: Inverse Fast Fourier Transform
ISI	: Inter Symbol Interference
MMSE	: Minimum Mean Squared Error
ML	: Maximum Likelihood
MSE	: Mean Square Error
OFDM	: Orthogonal Frequency Division Multiplexing
RS	: Reed Solomon
SC-CP	: Single Carrier Cyclic Prefix
SINR	: Signal to Interference Plus Noise Ratio
SNR	: Signal to Noise Ratio
TCM	: Trellis Coded Modulation
ZF	: Zero Forcing

CHAPTER 1

INTRODUCTION

In wireless communication systems the signal travels through multiple paths between transmitter and receiver. These paths occur because of the reflection, scattering, and diffraction of electromagnetic waves by walls, terrain, buildings, and other objects. At the receiver end, delayed and reflected replicas of the original signal are superimposed. This effect is termed as frequency selective fading. Frequency selective fading results in a distortion on the transmitted signal. Many methods are investigated in the literature to overcome the problem of multipath fading. Orthogonal frequency division multiplexing (OFDM) is a promising modulation technique over such channels. OFDM system converts a frequency selective fading channel into a set of parallel flat fading channels. Each frequency component of the signal experiences the same magnitude of fading over frequency flat subchannels so thus facilitates simpler equalization. When a signal sent through a frequency selective fading channel, some subcarriers may experience high attenuation whereas others may experience low attenuation. Although there are subcarriers with low attenuation and therefore have very few errors, the average bit error rate (BER) of an uncoded OFDM system is dominated by the subcarriers with the worst BER.

The effect of the OFDM system over fading channel can be thought as a set of frequency nonselective fading parallel channels. In this system each symbol is transmitted over a single flat subchannel that may encounter fading. And when channel nulls occur on these subchannels it becomes difficult to detect the symbols.

Reliability is an important requirement in communication systems. To achieve reliable communication, it is essential to reach low error probabilities. The error probability can be decreased by using diversity techniques such as repeating the symbols. While OFDM system converts a multipath fading channel into parallel flat fading channels the diversity available in multipath channels is lost. This loss of multipath diversity is usually recovered by using coding techniques. Classical solution is to apply an error correction code over the parallel channels and also over the OFDM symbols. In [1] and [2] different coded OFDM systems that improve system performance is reported.

Using precoder matrices to increase the diversity order and to recover loss of multipath diversity over fading channels is a relatively new approach [3], [4]. Different matrices are used as precoder matrices. Rotation code is one of these codes. Using rotation codes, the rotated version of the original signal constellation is send from the transmitter. This approach can be considered as an uncoded system because in this system there is no additional redundancy. Coding gain is obtained without spending additional bandwidth or power. In the literature different precoder matrices are used and their performance analysis are examined. In [5], [6], [7] antipodal paraunitary matrices are used as precoders in OFDM systems, the simulation and theoretical results are given. In [8] Vandermonde matrices are used as the precoder matrix, the performance and diversity order comparisons of the precoded OFDM and BCH coded OFDM are given.

Finding optimal precoder that minimizes the bit error rate (BER) is an important problem to achieve high performance in fading channels. In [9] the bit error rate minimization for OFDM transceivers with orthogonal precoders is considered. Increasing diversity order increases the system performance. By using precoder matrices the diversity order is increased and this comes with high performance. In [4] and [4] the diversity order is increased by using rotated QAM constellations.

Using rotated versions of constellations increase the performance. But the decoding stage also has an important effect on the performance. The maximum likelihood (ML), minimum mean squared error (MMSE), zero-forcing (ZF) receivers are used and their performance analysis have made in the literature. In [11], the zero-padding and cyclic prefix minimum BER precoders with zero forcing receivers are considered. Using iterative receivers instead of conventional MMSE or ZF receiver is another approach to increase the system performance. In

[12], the performance of MMSE successive interference cancellation receiver is considered. In [13], [14] some novel iterative receivers are proposed. In [15] a detection technique that performs a local ML search in the neighborhood of the output provided by the MMSE detector is proposed.

The main problem studied in this thesis is the problem of achieving reliable communication in fading channels. To accomplish this, the diversity concept is used. A different diversity technique, rotation coding is used for combating frequency selective fading. The object is to understand whether the OFDM systems that used precoder matrices is more effective than the conventional OFDM systems. Rotation coding can also be used with error correction codes for a better performance. Investigation of error-correction in addition to preoding is not within the content of this thesis. Another objective is to see the precoder effect on the simple receiver structures. Within this context the thesis consists of three main parts. In the first part the concept of rotation code is defined. In this part a brief description of diversity concept is given. Using rotation codes as precoder matrices increases the diversity order. From this point of view diversity order, signal to noise ratio (SNR) relations and the BER performance of the rotation code is discussed in this section. In the second part BER performance of precoded OFDM system and the BER performance of conventional OFDM system is compared. In the third chapter the simple receiver structures are discussed. The BER performance of different precoding matrices with zero-forcing (ZF) minimum mean squared error (MMSE) and maximum likelihood (ML) receiver are calculated.

CHAPTER 2

DIVERSITY

The system performance on a fading channel depends on SNR and therefore the strength of channel gains of the paths. If the path is not in a deep fade then reliable communication can be provided. In this thesis we investigate the fading problems in OFDM systems. To overcome fading diversity techniques are used with OFDM, the OFDM concept is given in the following chapter. In this chapter we first investigate the diversity concept itself.

The problem of being in a deep fade can be solved by using more than one path that fades independently from each other. This technique using many paths for signal transmission is called as diversity. There are diversity techniques operate over time, frequency or space. In this thesis only the signal space diversity is discussed. The other types of diversity are discussed in [16]. We will consider the type of Time Diversity and “Signal Space Diversity” or modulation diversity defined as in [4].

A straightforward way for providing time diversity is repeating the transmission symbols for L times. This concept is named as repetition coding. Time diversity does not require additional transmit power but by using this technique the data rate is decreased. A more sophisticated code that does not decrease the data rate is the constellation coding. These codes are considered in this chapter. The rate and diversity order comparisons of these two codes are given at the end of the chapter.

2.1 REPETITION CODING

Repetition coding is achieved by transmitting the same signal at different times. Consider the communication system over fading channel with BPSK symbols. In repetition coding, transmission symbol $\boldsymbol{x}$, will be send for L times.

Here L is the number of diversity branches. The first component x_1 is send in first symbol time, in the second symbol time again the first component x_1 is send and this continues same for L symbol times. So the received vector is,

$$\boldsymbol{y} = \boldsymbol{h} x_1 + \boldsymbol{n} \tag{2.1}$$

Here $\boldsymbol{y} = [y_1, y_2, \ldots, y_L]^T$, $\boldsymbol{h} = [h_1, h_2, \ldots\ldots, h_L]^T$, $\boldsymbol{n} = [n_1, n_2, \ldots, n_L]^T$ where $x_l = x_1 \quad l = 1, \ldots\ldots, L$ the transmitted symbols are BPSK symbols, $x_1 = \pm a$, $\boldsymbol{n}$ is AWGN with variance N_0, and $\boldsymbol{h}$ is the vector of Rayleigh fading channel coefficients. The performance of this system is often characterized by the diversity order associated with the probability of error.

We will use signal to noise ratio to find the probability of error. The general definition of signal to noise ratio is, [16]

$$SNR = \frac{\textit{average received signal energy per symbol time}}{\textit{noise energy per symbol time}}$$

In this system noise energy per symbol time is N_0 and signal energy is a^2. So the SNR is,

$$SNR = \frac{a^2}{N_0} \tag{2.2}$$

The error probability of detecting **x** is,

$$Q\left(\frac{a\|h\|}{\sqrt{N_0/2}}\right) = Q\left(\sqrt{2\|h\|^2 SNR}\right) \tag{2.3}$$

The quantity $\|h\|^2 SNR$ is the instantaneous received SNR and the Q function is the complementary cumulative distribution function of *N(0,1)* random variable. $Q(x)$ decays exponentially with x^2.

$$Q(x) < e^{\frac{-x^2}{2}}, \quad x>0$$

$$Q(x) > \frac{1}{\sqrt{2\pi}\,x}\left(1-\frac{1}{x^2}\right)e^{\frac{-x^2}{2}}, \qquad x>1 \tag{2.4}$$

The computations Q(1)=0.159 and Q(3)=0.00015 in equation (2.4) shows us how the tail of the Q function decays rapidly, [16].

Given $|h|^2\, SNR >> 1$, the conditional error probability is very small because, for x>1 the tail decays very rapidly and this corresponds to small error probability. When $|h|^2\, SNR$ is on the order of 1 or less, probability of error becomes significant. So we can define this high error region as the "deep fade" event, $|h|^2 < \frac{1}{SNR}$. Probability of this event is,

$$P\left[|h|^2\, SNR<1\right] = \int_0^{\frac{1}{SNR}} e^{-x}\,dx = \frac{1}{SNR} + O\left(\frac{1}{SNR^2}\right)$$

$$P\left[deep\,fade\right] \cong \frac{1}{SNR} \tag{2.5}$$

We average over the random gain h to find the overall error probability. Under Rayleigh fading with each gain h_l i.i.d $CN\left(0,1\right)$,

$$\|\boldsymbol{h}\|^2 = \sum_{l=1}^{L} |h_l|^2 \tag{2.6}$$

(2.6) is a sum of the squares of 2L independent real Gaussian random variables, each term $|h_l|^2$ being the sum of the squares of the real and imaginary parts of h_L.The density is given

$$f(x) = \frac{1}{(L-1)!}x^{L-1}e^{-x}, \qquad x \ge 0 \tag{2.7}$$

The average error probability can be computed to be, [16],

$$p_e = \int_0^\infty Q\left(\sqrt{2xSNR}\right) f(x)\, dx$$

$$p_e = \left(\frac{1-\mu}{2}\right)^L \sum_{l=0}^{L} \binom{L-1+l}{l} \left(\frac{1+\mu}{2}\right)^L, \;\; \mu = \sqrt{\frac{SNR}{1+SNR}} \quad (2.8)$$

At high SNR, Taylor series expansion yields,

$$\sqrt{\frac{SNR}{1+SNR}} = 1 - \frac{1}{2SNR} + \dots \quad (2.9)$$

using equation (2.9),

$$\left(\frac{1+\mu}{2}\right) = 1 - \frac{1}{4SNR} \quad (2.10)$$

in high SNR the second term of the right-hand side of equation (2.10) can be neglected. So equation (2.10) becomes;

$$\left(\frac{1+\mu}{2}\right) \cong 1 \quad (2.11)$$

$$\left(1 - \frac{\mu}{2}\right) = \frac{1}{4SNR} \quad (2.12)$$

$$\sum_{l=0}^{L-1} \binom{L-1+l}{l} = \binom{2L-1}{L} \quad (2.13)$$

using equations (2.11), (2.12) and (2.13) the overall probability of error is,

$$p_e = \binom{2L-1}{L}\left(\frac{1}{(4SNR)^L}\right) \tag{2.14}$$

As seen in equation (2.14), probability of error decreases by the L^{th} order of SNR. And in error probability curve this corresponds to a slope of –L in log-log plot as shown in Figure 2.1, [16].

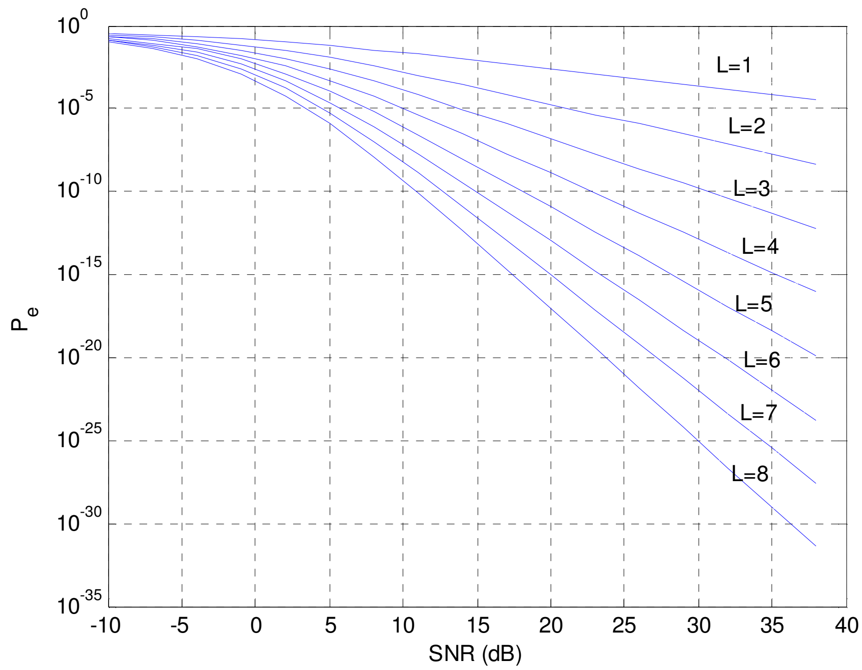

Figure 2.1 Error probability for different numbers of diversity branches L.

It is seen that the probability of error can be decreased significantly by increasing the diversity order.

The repetition coding is used to understand the effect of diversity. A repetition code simply repeats the same symbol over L symbol times. The problem with repetition coding is information rate is reduced by L that is 1 symbol is transmitted at every L symbol durations, to increase the reliability of the channel. We will focus on a scheme which is more sophisticated than repetition code providing the diversity gain at no rate loss. This scheme is called signal space diversity,[16].

In "Signal Space Diversity" the original signal constellation is mapped to a constellation of larger minimum Hamming distance (but at the same Euclidean distance). Hamming distance is defined as the number of components of a vector that are different from the components of other vector. Minimum Hamming distance between any two coordinate vectors of constellation points gives the diversity order. In other words diversity order of a multidimensional signal set is the minimum number of the distinct components between any two constellation points,[4].

To achieve signal space diversity a rotation matrix is used and this matrix rotates the signal constellation and increases the Hamming distance. This kind of matrix is named as constellation coding in [16] or rotation code in, [4].

2.2 CONSTELLATION CODING

Constellation coding is based on the idea of increasing the maximum number of distinct components between two vectors. And to perform this idea rotation codes are used as in [16].

To understand this coding scheme consider the following codewords,

$$\boldsymbol{x_A} = \begin{pmatrix} a \\ a \end{pmatrix}, \boldsymbol{x_B} = \begin{pmatrix} a \\ -a \end{pmatrix}, \boldsymbol{x_C} = \begin{pmatrix} -a \\ -a \end{pmatrix}, \boldsymbol{x_D} = \begin{pmatrix} -a \\ a \end{pmatrix} \tag{2.15}$$

The symbols $\boldsymbol{x_A}$ and $\boldsymbol{x_B}$ are being transmitted. The components of $\boldsymbol{x_A}$ are *(a,a)* and the components of $\boldsymbol{x_B}$ are *(a,-a)*.

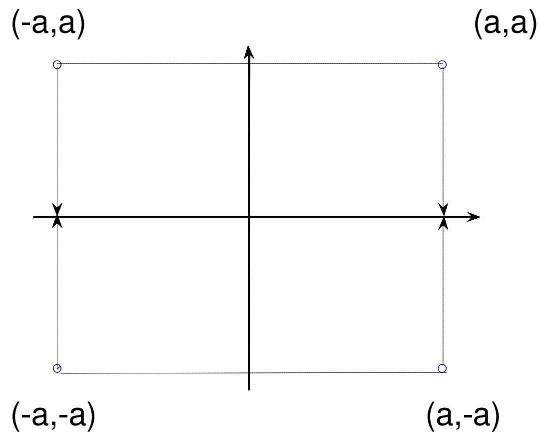

Figure 2.2 Codewords of repetition code

There is only one distinct component between the codewords $\boldsymbol{x}_A$ and $\boldsymbol{x}_B$, and this is the second component $-a$. It corresponds to the Hamming distance of 1 and the diversity order is 1. Consider the transmission of $\boldsymbol{x}_A$, if the second component of $\boldsymbol{x}_A$ is lost during the transmission we have $\boldsymbol{x}_A = (a, unknown)$. In this situation making a decision is very difficult because it may be $\boldsymbol{x}_A$ or $\boldsymbol{x}_B$. Probability of making a wrong decision is very high. If a rotated constellation was used as shown in Figure 2.3., the codewords are:

$$\boldsymbol{x}_A = \boldsymbol{R}\begin{bmatrix} a \\ a \end{bmatrix}, \quad \boldsymbol{x}_B = \boldsymbol{R}\begin{bmatrix} -a \\ a \end{bmatrix}, \quad \boldsymbol{x}_C = \boldsymbol{R}\begin{bmatrix} -a \\ -a \end{bmatrix}, \quad \boldsymbol{x}_D = \boldsymbol{R}\begin{bmatrix} a \\ -a \end{bmatrix} \tag{2.16}$$

where $\boldsymbol{R}$ is the rotation matrix:

$$\boldsymbol{R} = \begin{bmatrix} \cos\theta & -\sin\theta \\ \sin\theta & \cos\theta \end{bmatrix} \tag{2.17}$$

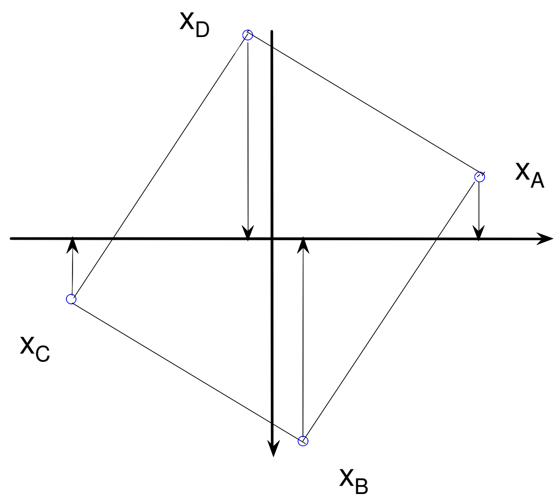

Figure 2.3 Codewords of rotation code

In this case none of the components of the codewords are the same. Both components in a symbol are distinct from components of another symbol. And this corresponds to the diversity order of 2.

The analysis of this case will be done as in [16]. Consider the communication over a fading channel again. The received signal is,

$$y_l = h_l x_l + n_l \qquad l = 1,2 \tag{2.18}$$

It is difficult to obtain an explicit expression for the exact error probability, so according to the union bound,

$$p_e = P(\boldsymbol{x_A} \rightarrow \boldsymbol{x_B}) + P(\boldsymbol{x_A} \rightarrow \boldsymbol{x_C}) + P(\boldsymbol{x_A} \rightarrow \boldsymbol{x_D}) \tag{2.19}$$

Here $p(\boldsymbol{x_A} \rightarrow \boldsymbol{x_B})$ is the pairwise error probability of detecting $\boldsymbol{x_B}$ when $\boldsymbol{x_A}$ is transmitted. In fading channel there are channel gains so the transmitted symbols become as,

$$\boldsymbol{u_A} = \begin{bmatrix} h_1 x_{A_1} \\ h_2 x_{A_2} \end{bmatrix} \qquad \boldsymbol{u_B} = \begin{bmatrix} h_1 x_{B_1} \\ h_2 x_{B_2} \end{bmatrix} \tag{2.20}$$

We are trying to detect transmit vector $\boldsymbol{u}$, equally likely to be $\boldsymbol{u}_A$ or $\boldsymbol{u}_B$. The received vector is,

$$\boldsymbol{y} = \boldsymbol{u} + \boldsymbol{n} \tag{2.21}$$

The Maximum Likelihood decision rule is to choose the nearest neighboring transmit symbol. It corresponds to choosing $\boldsymbol{u}_A$ when

$$\| \boldsymbol{y} - \boldsymbol{u}_A \| < \| \boldsymbol{y} - \boldsymbol{u}_B \| \tag{2.22}$$

Suppose $\boldsymbol{u}_A$ is transmitted so $\boldsymbol{y} = \boldsymbol{u}_A + \boldsymbol{n}$. Then an error occurs when $\|\boldsymbol{n}\| > \|\boldsymbol{n} + \boldsymbol{u}_A - \boldsymbol{u}_B\|$. The error probability is equal to,

$$P\left(\| \boldsymbol{n}\|^2 > \| \boldsymbol{n} + \boldsymbol{u}_A - \boldsymbol{u}_B \|^2\right) = P\left((\boldsymbol{u}_A - \boldsymbol{u}_B)^T \boldsymbol{n} < -\frac{\| \boldsymbol{u}_A - \boldsymbol{u}_B \|^2}{2}\right) \tag{2.23}$$

Thus the error probability can be written in compact notion as, [16]:

$$P\left(\boldsymbol{x}_A \rightarrow \boldsymbol{x}_B | h_1, h_2\right) = Q\left(\frac{\|\boldsymbol{u}_A - \boldsymbol{u}_B\|}{2\sqrt{N_0/2}}\right)$$

$$= Q\left(\sqrt{\frac{SNR\left(|h_1|^2 |d_1|^2 + |h_2|^2 |d_2|^2\right)}{2}}\right) \tag{2.24}$$

where $SNR = \dfrac{a^2}{N_0}$. We see that the error probability depends only on the Euclidean distance between $\boldsymbol{u}_A$ and $\boldsymbol{u}_B$.

$$\boldsymbol{d} := \frac{1}{a}(\boldsymbol{x}_A - \boldsymbol{x}_B) = \begin{bmatrix} 2\cos\theta \\ 2\sin\theta \end{bmatrix} \tag{2.25}$$

Equation (2.25) is the normalized difference between the codewords. According to the upper bound given in equation (2.4)

$$P\left(\boldsymbol{x}_A \rightarrow \boldsymbol{x}_B \mid h_1, h_2\right) \leq \exp\left(\frac{-SNR\left(|h_1|^2 |d_1|^2 + |h_2|^2 |d_2|^2\right)}{4}\right) \tag{2.26}$$

Averaging with respect to h_1 and h_2 under the independent Rayleigh fading assumption, we get

$$P(\boldsymbol{x}_\mathbf{A} \rightarrow \mathbf{x}_\mathbf{B}) \leq E_{h_1, h_2}\left[\exp\left(\frac{-SNR\left(|h_1|^2 |d_1|^2 + |h_2|^2 |d_2|^2\right)}{4}\right)\right]$$

$$P(\boldsymbol{x}_A \rightarrow \boldsymbol{x}_B) \leq \left(\frac{1}{1 + SNR\,|d_1|^2 / 4}\right)\left(\frac{1}{1 + SNR\,|d_2|^2 / 4}\right) \tag{2.27}$$

Here the moment generation function $E\{e^{sx}\} = \frac{1}{s}$ for $s<1$ is used. Consider the case of $d_1 = 0$ or $d_2 = 0$. In this case the diversity gain of the code is only 1, [16].

$$\boldsymbol{d} = \begin{pmatrix} d_1 \\ d_2 \end{pmatrix} = \frac{1}{a}\begin{pmatrix} x_{A_1} - x_{B_1} \\ x_{A_2} - x_{B_2} \end{pmatrix} \tag{2.28}$$

$$d_1 = 0 \Rightarrow x_{A_1} = x_{B_1} \qquad or \qquad d_2 = 0 \Rightarrow x_{A_2} = x_{B_2} \tag{2.29}$$

Only one of the components of the codewords is different. If they are both nonzero then at high SNR,

$$P(\boldsymbol{x}_A \rightarrow \boldsymbol{x}_B) = \frac{4}{SNR\,|d_1|^2}\,\frac{4}{SNR\,|d_2|^2} = \frac{16}{|d_1|^2 |d_2|^2} SNR^{-2} \tag{2.30}$$

Call $\delta_{AB} = |d_1 \, d_2|^2$ the squared product distance between $\boldsymbol{x_A}$ and $\boldsymbol{x_B}$. The squared product distance determines the pairwise error probability between the codewords.

$$p_e \le P\left(\boldsymbol{x_A} \rightarrow \boldsymbol{x_B}\right) + P\left(\boldsymbol{x_A} \rightarrow \boldsymbol{x_B}\right) + P\left(\boldsymbol{x_A} \rightarrow \boldsymbol{x_C}\right)$$

$$p_e \le 16\left(\frac{1}{\delta_{AB}} + \frac{1}{\delta_{AC}} + \frac{1}{\delta_{AD}}\right) SNR^{-2}$$

$$p_e \le \frac{48}{\min\limits_{j=B,C,D} \delta_{Aj}} SNR^{-2} \tag{2.31}$$

As long as $\delta_{ij} > 0$, the diversity gain is 2. The minimum squared product distance $\min\limits_{j=B,C,D} \delta_{Aj}$ determines the coding gain. To maximize the coding gain, the optimization will be done over θ, the angle of the rotation matrix components, [16].

$$\delta_{AB} = \left| \frac{1}{a}\left(x_{A_1} - x_{B_1}\right) \frac{1}{a}\left(x_{A_2} - x_{B_2}\right) \right|^2 \tag{2.32-a}$$

$$\delta_{AC} = \left| \frac{1}{a}\left(x_{A_1} - x_{C_1}\right) \frac{1}{a}\left(x_{A_2} - x_{C_2}\right) \right|^2 \tag{2.32-b}$$

$$\delta_{AD} = \left| \frac{1}{a}\left(x_{A_1} - x_{D_1}\right) \frac{1}{a}\left(x_{A_2} - x_{D_2}\right) \right|^2 \tag{2.32-c}$$

$$\delta_{AB} = \delta_{AD} = 4\sin^2 2\theta \qquad \delta_{AC} = 16\cos^2 2\theta \tag{2.33}$$

The angle θ that maximizes the minimum squared product distance makes,

$$\delta_{AB} = \delta_{AC} \quad and \quad \theta = \frac{1}{2}\tan^{-1} 2 \tag{2.34}$$

So

$$\min \delta_{ij} = 4\sin^2 2\left(\frac{1}{2}\tan^{-1} 2\right) = \frac{16}{5} \quad (2.35)$$

Now the bound in equation (2.31) becomes as,

$$p_e \leq \frac{48}{4\sin^2\left[\frac{2.1}{2}\tan^{-1} 2\right]} SNR^{-2} = 15SNR^{-2}$$

$$p_e \leq 15\, SNR^{-2} \quad (2.36)$$

As a summary, sending the same symbol for L times gives a diversity order of L. But repetition coding does not fully exploit the degrees of freedom available in the channel effectively. Reliable communication can be achieved by choosing L large enough. But the data rate is 1/L bits per symbol time and with increasing L, the data rate goes to zero.

To achieve high diversity order with high data rate different diversity technique is used. A suitable technique is the constellation rotation. The idea of rotating a constellation increases diversity order on the fading channels by spreading the information contained in each component over several components of the constellation paths. Rotation code also comes with coding gain. And this coding gain is proportional with the minimum product distance. This technique can be an alternative to other codes with combating fading because of its rate advantage. Because of this rate and diversity advantage of rotation code over repetition coding we will use rotation codes as precoders in OFDM system. To understand the effect of rotation code, in the next chapter the conventional OFDM system and rotation coded OFDM system and their BER comparisons are given.

CHAPTER 3

OFDM SYSTEM WITH ORTHOGONAL PRECODER

OFDM system converts the ISI channel into ISI free channels. In a multipath fading system, channel gains can be considered as random variables. Some OFDM subcarriers may be completely lost in case of deep fades. Although most subcarriers may be detected without errors, the overall bit error rate will be affected dominantly by the subcarriers that have small channel gains. This loss of multipath diversity is usually recovered by Forward Error Correction Coding [10]. In this thesis we use a different approach. In previous chapters it has seen that high diversity orders can be reached by rotation codes. And the BER can be decreased proportional to the diversity order. In the next chapter the rotation code is applied to the conventional OFDM system and the performance comparisons are made.

3.1 UNCODED OFDM SYSTEM

The block diagram of the OFDM system is shown in Figure 3.1 Assume that the number of subchannels is M. **s** is the vector of modulation symbols with dimension M by 1. Each input vector **s** is passed through M by M IFFT matrix, followed by the insertion of cyclic prefix and the parallel to serial operation. By insertion of cyclic prefix it is objected to remove inter-block interference. At the receiving end this cyclic prefix is removed. And the samples are blocked into M by 1 vector for M point FFT calculation. Typically an OFDM System is used with an interleaver. In this thesis, we assume that every parallel channel is independently faded. This assumption can be interpreted as in operation with very long interleaver or a system operating over very flat fading channel.

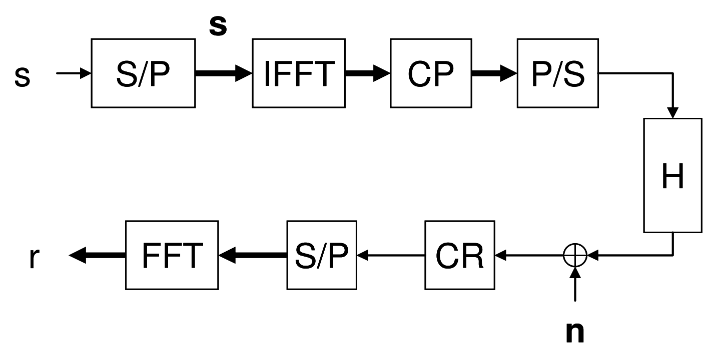

Figure 3.1 OFDM system block diagram

OFDM System avoids the inter symbol interference by implementing fast Fourier Transform (FFT) at the transmitter and inverse fast Fourier Transform (IFFT) at the receiver. This FFT implementation converts the channel with inter symbol interference (ISI) to the ISI free channel. To avoid interblock (IBI) and interchannel (ICI) interferences between successive IFFT processed blocks, a cyclic prefix (CP) of length greater than or equal to the channel order is inserted per block at the transmitter and discarded at the receiver, [17]. The CP converts the linear convolution to the cyclic convolution and the application of IDFT and DFT diagonalizes the channel matrix.

In serial transmission the transmitted symbols come to the receiver in the form of delayed and scaled replicas but OFDM transfers this multipath diversity to the frequency domain in the form of fading frequency response samples. Each OFDM subchannel gain is expressed as a linear combination of the dispersive channel taps. When the channel has nulls (deep fades) close to or on the FFT grid, reliable detection of the symbols carried by these faded subcarriers becomes difficult. For combating with this difficulty linear precoding will be used instead of classical coding techniques like convolutional codes, trellis-coded modulation (TCM) or coset codes, turbo codes, block codes (e.g., Reed–Solomon (RS) or Bose–Chaudhuri–Hocquenghem (BCH)). The idea of linear precoding or rotational coding is sending different linear combinations of the information symbols.

3.2 PRECODED OFDM SYSTEM

In this section the OFDM system with an orthogonal precoder is considered. Precoding is used in OFDM system with the assumption of there is no bandwidth and power allocation. The channels are Rayleigh fading i.i.d channels. In precoded OFDM system instead of sending uncoded symbols (one per subcarrier), the idea is to send different linear combinations of the information symbols on the subcarriers. This corresponds to signal space diversity as discussed in the previous sections. Different orthogonal precoders will be considered and the optimum precoder that guarantees the maximum diversity order without an essential decrease in transmission rate will be found. By performing pairwise error probability analysis, we will upper-bound the diversity order of OFDM transmissions over random frequency-selective fading channels. As expected the diversity order is directly related to the Hamming distance between coded symbols.

The precoded OFDM system is shown in Figure 3.2. Due to CP-insertion at the transmitter and CP-removal at the receiver, the dispersive channel is represented as an MxM circulant channel matrix **H**. Performing IFFT ($\mathbf{W}^{H}$) at the transmitter and FFT (**W**) at the receiver diagonalizes the circulant matrix **H**. So, we obtain the parallel ISI-free model for the OFDM symbol as

$$\boldsymbol{r}_{w} = \boldsymbol{D}_{H}\,\boldsymbol{u} + \boldsymbol{n} \qquad \boldsymbol{D}_{H} = \boldsymbol{W}\boldsymbol{H}\boldsymbol{W}^{H} \tag{3.1}$$

In a linearly precoded OFDM system different linear combinations of uncoded symbols are transmitted over different subcarriers. If a deep fade occurs in the channel, this only affects the linear combination of the transmitted symbols. The receiver can still recover the transmitted symbols from the data received on the other subcarriers. In order to see precoder effect on OFDM system we consider the Hamming distance. As we have discussed before The Hamming distance between two vectors $\boldsymbol{x}$ and $\boldsymbol{x}'$ is defined as the number of nonzero entries in the vector $\boldsymbol{x}_e = \boldsymbol{x} - \boldsymbol{x}'$.

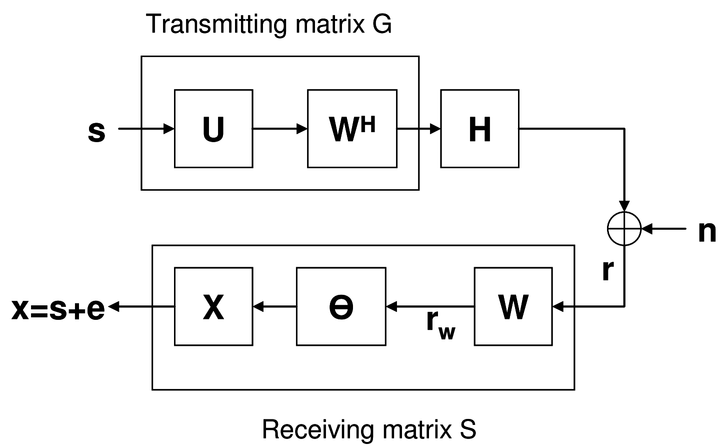

Figure 3.2 OFDM system with precoder

Consider an OFDM system with 2 parallel channels. And the channel coefficients are α_1 and α_2. The transmission symbols are BPSK symbols $b_1, b_2 = \pm 1$ and the precoder matrix is $\begin{bmatrix} 1 & -1 \\ 1 & 1 \end{bmatrix}$. In precoded system we send $\begin{bmatrix} 1 \\ 1 \end{bmatrix} b_1$ through the first channel with the coefficient α_1 (first component of the vector is multiplied by α_1) and similarly through the second channel with the coefficient α_2. So the received vector is,

$$\boldsymbol{r} = \begin{bmatrix} \alpha_1 \\ \alpha_2 \end{bmatrix} b_1 + \begin{bmatrix} \alpha_1 \\ -\alpha_2 \end{bmatrix} b_2 = \begin{bmatrix} \alpha_1 & \alpha_1 \\ \alpha_2 & -\alpha_2 \end{bmatrix} \begin{bmatrix} b_1 \\ b_2 \end{bmatrix} \qquad (3.2)$$

$\boldsymbol{A} = \begin{bmatrix} \alpha_1 & \alpha_1 \\ \alpha_2 & -\alpha_2 \end{bmatrix}$ and $b = \begin{bmatrix} b_1 \\ b_2 \end{bmatrix}$. We have two channels and the transmitted vectors may be, $\begin{bmatrix} 1 \\ 1 \end{bmatrix}, \begin{bmatrix} 1 \\ -1 \end{bmatrix}, \begin{bmatrix} -1 \\ 1 \end{bmatrix}, \begin{bmatrix} -1 \\ -1 \end{bmatrix}$. In precoded system these transmitted vectors will become into, $\boldsymbol{A}\begin{bmatrix} 1 \\ 1 \end{bmatrix}, \boldsymbol{A}\begin{bmatrix} 1 \\ -1 \end{bmatrix}, \boldsymbol{A}\begin{bmatrix} -1 \\ 1 \end{bmatrix}, \boldsymbol{A}\begin{bmatrix} -1 \\ -1 \end{bmatrix}$.

Consider the case $\begin{bmatrix} 1 \\ 1 \end{bmatrix}$ is send and $\begin{bmatrix} 1 \\ -1 \end{bmatrix}$ is detected. In this case the error vector is

$$\boldsymbol{e} = \boldsymbol{A}\left(\begin{bmatrix}1\\1\end{bmatrix} - \begin{bmatrix}1\\-1\end{bmatrix}\right) = \boldsymbol{A}\begin{bmatrix}0\\2\end{bmatrix}$$

$$\boldsymbol{e} = \begin{bmatrix}\alpha_1\\-\alpha_2\end{bmatrix}2 \tag{3.3}$$

We have defined the Hamming distance as the number of nonzero elements in the difference vector. So in the precoded OFDM system the Hamming distance of ***e*** is 2. It corresponds to the diversity order of 2.

If we consider the uncoded system because of the cyclic prefix and the FFT implementation we have 2x2 diagonal channel matrix as $\begin{bmatrix}\alpha_1 & 0\\0 & \alpha_2\end{bmatrix}$. We send the transmission symbols through the channels again and have the received vector as

$$\boldsymbol{r} = \begin{bmatrix}a_1 & 0\\0 & \alpha_2\end{bmatrix}\begin{bmatrix}b_1\\b_2\end{bmatrix} \tag{3.4}$$

Here $\boldsymbol{A} = \begin{bmatrix}\alpha_1 & 0\\0 & \alpha_2\end{bmatrix}$ *and* $\boldsymbol{b} = \begin{bmatrix}b_1\\b_2\end{bmatrix}$. And the error of deciding $\begin{bmatrix}1\\-1\end{bmatrix}$ when $\begin{bmatrix}1\\1\end{bmatrix}$ is transmitted is,

$$\boldsymbol{e} = \boldsymbol{A}\left(\begin{bmatrix}1\\1\end{bmatrix} - \begin{bmatrix}1\\-1\end{bmatrix}\right) = \boldsymbol{A}\begin{bmatrix}0\\2\end{bmatrix}$$

$$\boldsymbol{e} = \begin{bmatrix}0\\\alpha_2\end{bmatrix}2 \tag{3.5}$$

The number of nonzero elements in the vector ***e*** is 1 and this corresponds to the diversity order of 1. Hence the uncoded OFDM system has the diversity order of 1.

We can see that the rotation code increases the diversity order also in the OFDM system. Using this rotation codes the performance of the OFDM system can be increased with low complexity.

The receiver structure is also important in this system. In order to recover the precoded OFDM data various detection techniques can be applied. Each of these techniques presents different complexity versus BER tradeoffs. The maximum likelihood (ML) detector chooses the nearest codeword to the received vector as the most likely transmitted codeword. So when rotation code is used with ML receiver it is able to get both the diversity and coding gain. However its computational complexity is exponential in the precoder size. Minimum Mean Square Error (MMSE) and Zero forcing (ZF) detectors can decrease this computational complexity. In the next chapters we will compare the BER performance of these detectors in precoded OFDM system. To understand the concept clearly a brief description about these receivers and MSE-BER relations in these receivers is given.

CHAPTER 4

RECEIVER STRUCTURES FOR PRECODED OFDM SYSTEM

The chapter 2 is concentrated on the problem of multipath fading in wireless channels. Diversity concept is considered as a solution for this problem. In chapter 3 the rotation code which brings diversity gain with high code rate is offered to overcome the problem of multipath fading. The rate and diversity order comparisons are given for repetition code and rotation code in chapter 3. All of the performance analysis considered for the OFDM system. The main problem is how this rotation code behaves on simple receiver structures as ML, MMSE and ZF. In this chapter, brief descriptions of the ZF and MMSE receivers are given. The BER performances of different precoder matrices on different receivers are calculated.

4-1 ZERO FORCING RECEIVERS

Zero forcing receivers are designed for eliminating interference completely. If **H** is the channel matrix and $\mathbf{S_{ZF}}$ is the Zero-forcing receiver matrix, ZF detector chooses $\mathbf{S_{ZF}}$ as $\mathbf{S_{ZF}H=I}$. If the channel matrix is not an invertible matrix Moore-Penrose pseudoinverse of **H** is used. It is given as,

$$H^{+} = \left(\mathbf{H^H H}\right)^{-1} \mathbf{H^H} \tag{4.1}$$

This kind of receiver cancels all ISI, but may increase the noise. Consider the communication over channel **H**. Then the received signal is;

$$\boldsymbol{r} = \boldsymbol{H}\boldsymbol{u} + \boldsymbol{n} \tag{4.2}$$

Assume the case that **H** is full rank square matrix. In this case the inverse of the channel matrix exists and $\boldsymbol{S_{ZF}} = \mathbf{H}^{+}$. When we multiply both sides of equation (4.2) with $\boldsymbol{S_{ZF}}$, we have,

$$\boldsymbol{H}^{+}\boldsymbol{r} = \boldsymbol{u} + \boldsymbol{H}^{+}\boldsymbol{n} \tag{4.3}$$

The noise is still Gaussian and the received symbol can be decoded by finding the closest constellation point of $\boldsymbol{H}^{-1}\boldsymbol{r}$. However the variance of noise in the $\boldsymbol{H}^{+}\boldsymbol{n}$ may be more than the power of the original noise $\boldsymbol{n}$. The covariance matrix of the noise can be calculated as,

$$\begin{aligned}\boldsymbol{H}^{+}\boldsymbol{R}_{n}\left(\boldsymbol{H}^{+}\right)^{\boldsymbol{H}} &= N_0\boldsymbol{H}^{+}\left(\boldsymbol{H}^{+}\right)^{\boldsymbol{H}} \\ &= N_0\left(\boldsymbol{H}^{\boldsymbol{H}}\boldsymbol{H}\right)^{-1}\boldsymbol{H}^{\boldsymbol{H}}\boldsymbol{H}\left(\boldsymbol{H}^{\boldsymbol{H}}\boldsymbol{H}\right)^{-1} \\ &= N_0\left(\boldsymbol{H}\boldsymbol{H}^{\boldsymbol{H}}\right)^{-1}\end{aligned} \tag{4.4}$$

The noise variance N_0 is increased by the diagonal elements of $\left(\boldsymbol{H}\boldsymbol{H}^{\boldsymbol{H}}\right)^{-1}$. If the channel **H** is sharply attenuated at any frequency within the bandwidth of interest, the noise power will be significantly increased. In the next chapters the performance of precoding on ZF equalization is considered.

4-2 MINIMUM MEAN SQUARE ERROR (MMSE) RECEIVERS

In MMSE estimation, the object is to minimize average mean square error between the estimated and transmitted symbols. MMSE detector can balance the noise enhancement and the interference cancellation. Consider the communication system above. The MMSE detector minimizes the sum

$$\boldsymbol{MSE} = \boldsymbol{E}\left\{|\boldsymbol{S}_{\boldsymbol{MMSE}}\boldsymbol{r} - \boldsymbol{u}|^{2}\right\} \tag{4.5}$$

$$\begin{aligned}\boldsymbol{MSE} &= \boldsymbol{E}\left\{\left(\boldsymbol{S}_{\boldsymbol{MMSE}}\boldsymbol{r} - \boldsymbol{u}\right)\left(\boldsymbol{S}_{\boldsymbol{MMSE}}\boldsymbol{r} - \boldsymbol{u}\right)^{\boldsymbol{H}}\right\} \\ &= \boldsymbol{S}_{\boldsymbol{MMSE}}\boldsymbol{R}_{r}\boldsymbol{S}_{\boldsymbol{MMSE}}^{\boldsymbol{H}} + \boldsymbol{I} - \boldsymbol{S}_{\boldsymbol{MMSE}}\boldsymbol{H} - \boldsymbol{H}^{\boldsymbol{H}}\boldsymbol{S}_{\boldsymbol{MMSE}}^{\boldsymbol{H}} \\ &= \left(\boldsymbol{S}_{\boldsymbol{MMSE}} - \boldsymbol{H}^{\boldsymbol{H}}\boldsymbol{R}_{r}^{-1}\right)\boldsymbol{R}_{r}\left(\boldsymbol{S}_{\boldsymbol{MMSE}} - \boldsymbol{H}^{\boldsymbol{H}}\boldsymbol{R}_{r}^{-1}\right)^{\boldsymbol{H}} + \boldsymbol{I} - \boldsymbol{H}^{\boldsymbol{H}}\boldsymbol{R}_{r}^{-1}\boldsymbol{H}\end{aligned}$$

$$= \left(S_{MMSE} - H^{H} R_r^{-1}\right) R_r \left(S_{MMSE} - H^{H} R_r^{-1}\right)^{H} + N_0\left(H^{H} H + N_0 I\right)^{-1} \quad (4.6)$$

To achieve the minimum MSE the first term of equation (4.6),

$$\left(S_{MMSE} - H^{H} R^{-1}\right) R_r^{-1} \left(S_{MMSE} - H^{H} R_r^{-1}\right)^{H} \quad (4.7)$$

that contains S_{MMSE} term can be made zero. So the MMSE solution is

$$S_{MMSE} = H^{H} R_r^{-1} \quad (4.8)$$

$$R_r = E\left\{(Hu + n)(Hu + n)^{H}\right\}$$

$$R_r = HH^{H} + N_0 \mathbf{I} \quad (4.9)$$

Using equation (4.8) in (4.7) and taking R_U as I, the MMSE receiver becomes,

$$S_{MMSE} = H^{H}\left(HH^{H} + N_0 I\right)^{-1} \quad (4.10)$$

In the following sections the performance of precoding on MMSE equalization is considered.

4-3 ZERO FORCING RECEIVERS WITH ORTHOGONAL RECODER

In this part the effect of precoder on zero forcing receiver is considered. The communication system uses OFDM modulation and the receiver structure is ZF. The system is shown in Figure 4.1.

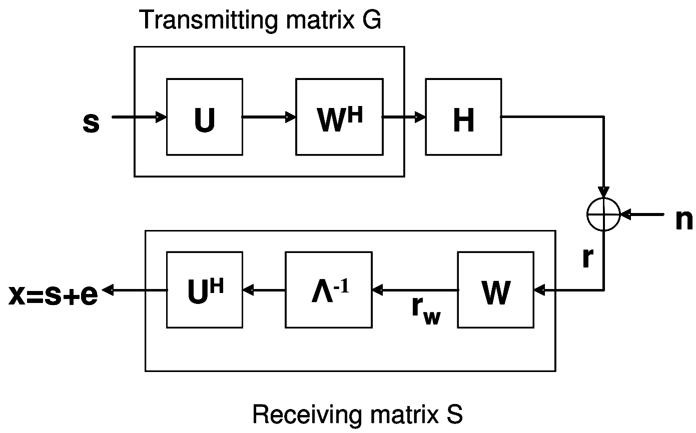

Figure 4.1 Precoded OFDM system with ZF receiver

In the system shown in Figure 4.1, the precoding matrix, $\boldsymbol{U}$ is unitary with $\boldsymbol{U}^H \boldsymbol{U} = \boldsymbol{I}$. $\boldsymbol{W}$ is the DFT matrix. Here $\boldsymbol{H}$ is circular convolutionoal matrix and, $\boldsymbol{WHW}^H = diag\left(P_0, \ldots P_{M-1}\right) = \Lambda$. Here $P_0, P_1, \ldots, P_{M-1}$ are the M-point DFT of the channel impulse response. The transmitting matrix in the transceiver is $\boldsymbol{G} = \boldsymbol{W}^H \boldsymbol{U}$. The input **r** to the receiver can be represented as

$$\boldsymbol{r} = \boldsymbol{HW}^H \boldsymbol{Us} + \boldsymbol{n}$$

$$\boldsymbol{r} = \boldsymbol{HGs} + \boldsymbol{n} \tag{4.11}$$

The zero forcing equalizer removes all ISI. The equalizer to accomplish this is given by

$$\boldsymbol{S}_{ZF} = (\boldsymbol{HG})^{-1} = \left(\boldsymbol{HW}^H \boldsymbol{U}\right)^{-1}$$

$$\boldsymbol{S}_{ZF} = \boldsymbol{U}^H \boldsymbol{W} \boldsymbol{H}^{-1} \tag{4.12}$$

$\boldsymbol{S}_{ZF}$ exists provided that the inverses in (4.12) exists since $\boldsymbol{U}$ and $\boldsymbol{W}$ are unitary matrices, their inverse exist and $\boldsymbol{H}^{-1}$ exists if Λ has all non-zero diagonal elements. So in Figure 4.1, $\boldsymbol{X} = \boldsymbol{U}^{T}$. For the communication system shown in Figure 4.1 when $\boldsymbol{s}$ is transmitted the decoded vector $\boldsymbol{x}$ is given by;

$$\boldsymbol{x} = \boldsymbol{S}_{ZF}\,\boldsymbol{r} = \boldsymbol{S}_{ZF}\,(\boldsymbol{HG})\,s + \boldsymbol{S}_{ZF}\,\boldsymbol{n}$$

$$\boldsymbol{x} = \boldsymbol{s} + \boldsymbol{U}^{H}\,\Lambda^{-1}\,\boldsymbol{W}\boldsymbol{n} \tag{4.13}$$

This is the expression of the received vector in zero-forcing receiver system. To find the effect of precoding over performance of the OFDM system, the BER criteria is used. To compare the performance of uncoded and precoded OFDM systems it is necessary to calculate the bit error rates (BER) of these two systems. So analyzing the noise vector is essential.

The channel noise $\boldsymbol{n}$ is AWGN with variance N_0. The modulation scheme is QPSK and the modulation symbols are $s_k = \pm\sqrt{\frac{\varepsilon_s}{2}} \pm j\sqrt{\frac{\varepsilon_s}{2}}$ with symbol energy ε_s. The receiver output vector is $\boldsymbol{x}$ and the output error vector is $\boldsymbol{e} = \boldsymbol{x} - \boldsymbol{s}$ as shown in Figure 4.1.

To analyze the noise vector consider the receiver block diagram in Figure 4.2, $\boldsymbol{n}$ is the M by 1 vector of the noise process. The elements of $\boldsymbol{n}$ are uncorrelated Gaussian random variables with variance N_0. The elements of $\mu = \boldsymbol{W}\boldsymbol{n}$ stay uncorrelated Gaussian random variables with variance N_0, because $\boldsymbol{W}$ is a unitary matrix.

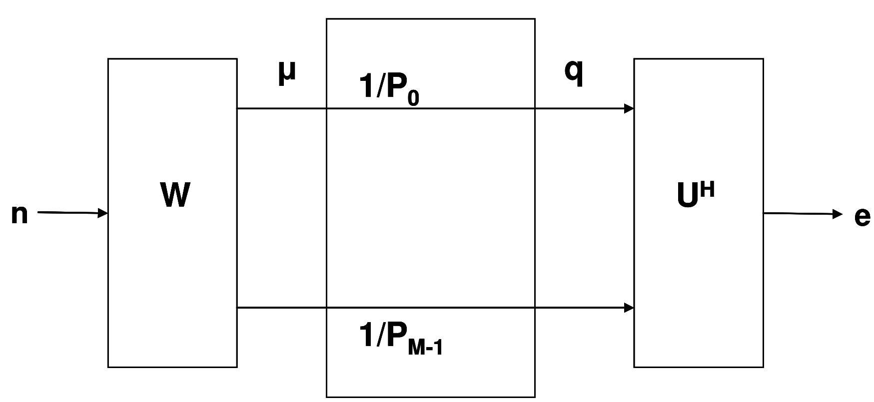

Figure 4.2 Noise path at a zero forcing receiver.

The variance of the k^th element of the noise vector q is given by,

$$\sigma_{qk}^2 = \frac{N_0}{|P_k|^2} \tag{4.14}$$

$\boldsymbol{U} = [\boldsymbol{u_1}\ \boldsymbol{u_2} \ldots \boldsymbol{u}_M]$ and the output noise $\boldsymbol{e} = \boldsymbol{U}^{\boldsymbol{H}}\boldsymbol{q}$ in the vector form. The i^th component of the error vector is given by

$$e_i = \boldsymbol{u_i^H}\,\boldsymbol{q} = \sum_{k=0}^{M-1} u_{k,i}^*\ q_k \tag{4.15}$$

$u_{k,i}$ denotes the (k,i)^th component of **U** matrix. According to equation (4.15), the noise variance of this subchannel is

$$\sigma_{e_i}^2 = N_0 \sum_{k=0}^{M-1} \frac{|u_{k,i}|^2}{|P_k|^2} \qquad for\, i = 0, \ldots\ldots, M-1 \tag{4.16}$$

The real and imaginary parts of e_i have equal variance. The SNR of the i^th subchannel is

$$SNR_i = \frac{\varepsilon_s}{\sigma_{e_i}^2} \tag{4.17}$$

$$SNR = \frac{\varepsilon_s}{N_0 \cdot \sum_{k=0}^{M-1} \frac{|u_{k,i}|^2}{|P_k|^2}} = \frac{\gamma}{\sum_{k=0}^{M-1} \frac{|u_{k,i}|^2}{|P_k|^2}} \qquad where\ \ \gamma = \frac{\varepsilon_s}{N_0} \tag{4.18}$$

As the precoder matrix **U** is unitary, $\sum_{k=0}^{M-1} |u_{k,i}|^2 = \sum_{i=0}^{M-1} |u_{i,k}|^2 = 1$ Then the average mean square error (MSE) is

$$MSE_{avg} = \frac{1}{M} \sum_{i=0}^{M-1} \sigma_{e_i}^2 = \frac{1}{M} \sum_{i=0}^{M-1} N_0 \sum_{k=0}^{M-1} \frac{|u_{k,i}|^2}{|P_k|^2}$$

$$= \frac{N_0}{M} \sum_{i=0}^{M-1} \frac{1}{|P_i|^2} \tag{4.19}$$

From the equation (4.19) it is clear that the average MSE is independent of the precoder matrix **U**. For performance comparison, consider BER of the i^{th} subchannel. For QPSK modulation the BER of the i^{th} subchannel is

$$BER_i = Q\left(\sqrt{SNR_i}\right) = Q\left(\sqrt{\frac{\varepsilon_s}{\sigma_{e_i}^2}}\right) \tag{4.20}$$

The average BER is

$$BER_{avg} = \frac{1}{M} \sum_{i=0}^{M-1} Q\left(\sqrt{\frac{\varepsilon_s}{\sigma_{e_i}^2}}\right) \tag{4.21}$$

The average BER is proportional to the noise variance of the subchannels. And the subchannel noise variance is proportional to the precoder matrix components. So selection of the precoding matrix affects the BER performance of the communication system.

We make the analytical BER analysis for two different cases, [18]. In one of these cases, the identity matrix is used as precoder and in the other one, DFT matrix is used as precoder.

Consider the selection of **U** is identity, **U=I.** This system corresponds to the system with no precoder namely the conventional OFDM system. The subchannel noise variance for this system is,

$$\sigma_{e_i}^2 = \frac{N_0}{|P_i|^2} \qquad i = 0, \ldots \mathrm{M} - 1 \tag{4.22}$$

SNR for the ith subchannel is given as,

$$SNR_i = \frac{\varepsilon_S}{\sigma^2_{e_i}} = \frac{\varepsilon_S}{\frac{N_o}{|P_i|^2}} = \gamma |P_i|^2 \qquad where \qquad \gamma = \frac{\varepsilon_S}{N_0} \tag{4.23}$$

The BER of the conventional OFDM system is,

$$BER_{avg} = \frac{1}{M} \sum_{i=0}^{M-1} Q\left(\sqrt{\gamma |P_i|^2}\right) \tag{4.24}$$

In the second case the precoder matrix is chosen as **U=W** (DFT matrix) then the transmitting matrix in Figure 4.1 becomes

$$\mathbf{G} = \mathbf{W}^{\mathrm{H}}\mathbf{W} = \mathbf{I} \tag{4.25}$$

The unitary matrix $\mathbf{U}^{\mathrm{H}}$ which is added to the receiver is now $\mathbf{W}^{\mathrm{H}}$. The resulting system is shown in Figure 4.2. This system can be seen as a single carrier communication system with cyclic prefix (SC-CP) is added. [9]. The SC-CP system can be thought as a precoded OFDM system with a precoder **U=W**, [18]

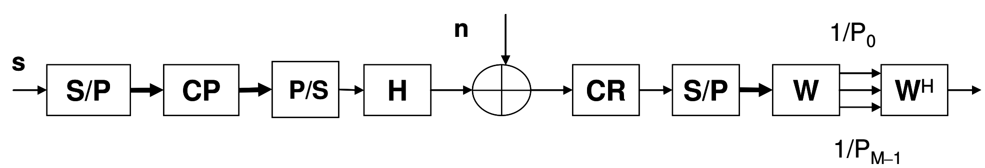

Figure 4.3 SC-CP System Block Diagram

Now consider the noise variance in SC-CP system. The noise path is shown in Figure 4.3. All the elements in the DFT matrix have the magnitude $\frac{1}{\sqrt{M}}$. The output noise is,

$$e_i = \frac{1}{\sqrt{M}} \sum_{k=0}^{M-1} q_k \tag{4.26}$$

and the noise variance of the SC-CP system is,

$$\sigma_{e_i}^2 = \frac{N_0}{M}\sum_{k=0}^{M-1}\frac{1}{|P_k|^2} \qquad for\, i = 0,1,\ \ldots\ldots\ldots, M-1 \qquad (4.27)$$

From the variance calculation, it is clear that the noise variances for all parallel subchannels are the same. The average MSE of the system is,

$$MSE_{avg} = \sigma_{e_i}^2 \qquad (4.28)$$

The SNR of the subchannels is,

$$SNR_i = \frac{\varepsilon_s}{\sigma_{e_i}^2} \qquad (4.29)$$

The BER of the SC-CP system can be written as

$$BER_i = Q\left(\sqrt{SNR_i}\right) \qquad (4.30)$$

The BER performance of the precoded system is determined by subchannel SNRs. [18]

Up to now the analytical results of SNR and BER criteria for two different precoder matrices are given. These precoder matrices are used on OFDM system with zero forcing equalizer. For different choices of **U** the noise variances are distributed differently and related to these variances SNR and BER performances differ.

To analyze BER performance we can use the function f that is defined as $f(x) = Q\left(\frac{1}{\sqrt{x}}\right)$. Here $f(x)$ corresponds to SNR value and x is MSE value. [18]. (Additional information about the SNR- MSE relations on ZF receiver can be found in Appendix B.) The BER performance can be seen from the behavior of f function. The convexity analysis of f function which is from [18], can be found in Appendix C.

According to the convexity analysis the f function has two regions. In high SNR region the function is convex, and in low SNR region the function is concave. The conventional OFDM system (**U=I**) is the optimal solution for low

SNR region because the BER is minimum in this region. On the contrary when all the subchannels operate in the convex region i.e., in high SNR region, the OFDM system has the largest BER. In this region we need additional precoder as in SC-CP system. From this result, it can be seen that using precoder in ZF-receiver system is not effective for all SNR regions. [18]

From above calculations it is obvious that selecting optimal precoder matrix and receiver structure gives a better BER solution than conventional OFDM, at no loss of rate. In the next section the same calculations are given for MMSE receiver. Then the BER results are compared.

4-4 MMSE RECEIVER WITH ORTHOGONAL PRECODER

In this part the OFDM system with an MMSE receiver is considered. The BER and SNR analysis of the system are given in this section. According to the analysis it is seen that the precoded OFDM system with MMSE receiver has better performance than the precoded OFDM system with ZF receiver.

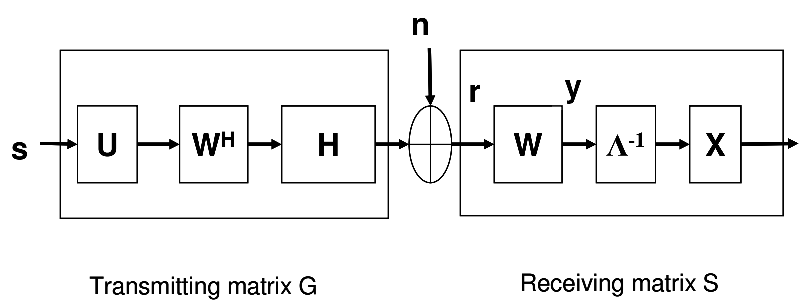

Figure 4.4 Precoded OFDM System with MMSE receiver

Consider Figure 4.4 again, in this part we have MMSE receiver at the place of **X**. We have called the output of the block **W** as the **y** vector:

$$\boldsymbol{y} = \boldsymbol{W H W}^{H} \boldsymbol{U s} + \boldsymbol{W n}$$

$$\boldsymbol{y} = \Lambda \boldsymbol{U s} + \boldsymbol{w} \qquad (4.31)$$

where Λ is the diagonal matrix with entries $\{P_0, \ldots\ldots P_{M-1}\}$ and $\boldsymbol{w}$ is noise vector with covariance matrix $N_0\boldsymbol{I}$. We would like to find $\boldsymbol{S}_{MMSE}$ such that $E\{\|\boldsymbol{S}_{MMSE}\boldsymbol{y}-\boldsymbol{s}\|^2\}$ is minimized using (4.8) and (4.9); we can immediately find $\boldsymbol{S}_{MMSE}$ from 4.8 as follows:

$$\boldsymbol{S}_{MMSE} = \boldsymbol{E}_s\left(\boldsymbol{U}^H\Lambda^H\right)\left(\Lambda\boldsymbol{U}\boldsymbol{U}^H\Lambda^H\boldsymbol{E}_S+\boldsymbol{N}_0\boldsymbol{I}\right)^{-1}$$

$$=\boldsymbol{E}_s\boldsymbol{U}^H\Lambda^H\left(\Lambda\Lambda^H\boldsymbol{E}_s+\boldsymbol{N}_0\boldsymbol{I}\right)^{-1} \tag{4.32}$$

The decoded vector is

$$\boldsymbol{x}=\boldsymbol{S}_{MMSE}\boldsymbol{y}=\boldsymbol{U}^H\underbrace{E_s\Lambda^H\left(\Lambda\Lambda^H E_s+N_0\boldsymbol{I}\right)^{-1}\Lambda}_{\boldsymbol{D}}\boldsymbol{U}\boldsymbol{s}+\boldsymbol{U}^H\Lambda^H\left(\Lambda\Lambda^H+N_0\boldsymbol{I}\right)^{-1}\boldsymbol{w} \tag{4.33}$$

Calling the diagonal matrix in the equation (4.33) as $\boldsymbol{D}$, the diagonal entries are;

$$\boldsymbol{D}=diag\left(E_s\frac{|P_0|^2}{N_0+E_s|P_o|^2},\ldots\ldots\ldots\ldots\ldots\ldots\ldots,E_s\frac{|P_{M-1}|^2}{N_0+E_s|P_{M-1}|^2}\right) \tag{4.34}$$

We get the following error vector,

$$\boldsymbol{e}=\boldsymbol{x}-\boldsymbol{s}=\boldsymbol{U}^H\boldsymbol{D}\boldsymbol{U}\boldsymbol{s}+\boldsymbol{U}^H\Lambda\boldsymbol{W}\boldsymbol{n}-\boldsymbol{s}$$

$$\boldsymbol{e}=\boldsymbol{U}^H(\boldsymbol{D}-\boldsymbol{I})\boldsymbol{U}\boldsymbol{s}+\boldsymbol{U}^H\Lambda\boldsymbol{W}\boldsymbol{n} \tag{4.35}$$

$$MSE_i=E\{|e_i|^2\}=\sum_{k=0}^{M-1}|u_{k,i}|^2\frac{\varepsilon_s}{\left(1+\gamma|P_k|^2\right)^2}+\sum_{k=0}^{M-1}|u_{k,i}|^2\frac{N_0\gamma^2|P_k|^2}{\left(1+\gamma|P_k|^2\right)^2}$$

$$MSE_i=\sum_{k=0}^{M-1}|u_{k,i}|^2\frac{\varepsilon_s}{1+\gamma|P_k|^2} \tag{4.36}$$

The average MSE is,

$$MSE_{avg} = \frac{1}{M}\sum_{i=0}^{M-1} MSE_i = \frac{1}{M}\sum_{i=0}^{M-1}\sum_{k=0}^{M-1} |u_{k,i}|^2 \frac{\varepsilon_s}{1+\gamma|P_k|^2}$$

$$MSE_{avg} = \frac{1}{M}\sum_{k=0}^{M-1} |u_{k,i}|^2 \frac{\varepsilon_s}{1+\gamma|P_k|^2} \tag{4.37}$$

The SINR of the ith estimation of the coefficient becomes,

$$\begin{aligned}(SNR)_i = \frac{1}{(MSE)_i \big/ \varepsilon_s} - 1 &= \frac{1}{\sum_{k=0}^{M-1} \frac{|u_{k,i}|^2}{1+\gamma|P_k|^2}} \\ &= \frac{\left(\sum_{k=0}^{M-1} |u_{k,i}|^2 \frac{\gamma|P_k|^2}{1+\gamma|P_k|^2}\right)}{\left(\sum_{k=0}^{M-1} \frac{|u_{k,i}|^2}{1+\gamma|P_k|^2}\right)}\end{aligned} \tag{4.38}$$

Additional information about this relation, $(SNR)_i = \frac{1}{(MSE)_i \big/ \varepsilon_s} - 1$, between MSE and SINR in MMSE receiver is given in Appendix B.

The BER calculation depends on the modulation scheme. The modulation scheme used in this system is QPSK. So the ith subchannel BER is

$$BER_i = Q\left(\sqrt{SINR_i}\right) = Q\left(\sqrt{\frac{1}{\left(\eta MSE\right)_i} - 1}\right) \tag{4.39}$$

where $\left(\eta MSE\right)_i = \frac{(MSE)_i}{\varepsilon_s}$ is the normalized MSE. Using the MSE-SINR relation in an MMSE receiver the computation complexity of BER will be decreased. Define a function h as, $h\left(\eta MSE\right) = Q\left(\sqrt{SNR_i}\right)$. Then the subchannel BER is,

$$BER_{avg} = \frac{1}{M}\sum_{i=0}^{M-1} h\left(\eta MSE\right)$$

$$BER_{avg} = \frac{1}{M} \sum_{i=0}^{M-1} h\left(\sum_{k=0}^{M-1} \frac{|u_{k,i}|^2}{1 + \gamma |P_k|^2} \right) \tag{4.40}$$

When the precoder matrix is identity, i.e., **U=I,** the system becomes the conventional OFDM system. In the conventional OFDM system, the subchannel SINR is,

$$SINR_i = \gamma |P_i|^2 \tag{4.41}$$

and it is the same SNR as in the zero forcing case. The MMSE and the ZF receiver gives the same performance in conventional OFDM system. The BER of the OFDM system is,

$$BER_{avg,OFDM} = \frac{1}{M} \sum_{i=0}^{M-1} h\left(\frac{1}{1 + \gamma |P_i|^2} \right) \tag{4.42}$$

When the precoder matrix **U** is DFT matrix then $|u_{k,i}| = \frac{1}{\sqrt{M}} \;\; \forall k,i$ and the system becomes SC-CP system. The BER is from equations 4.36 and 4.40;

$$BER_{avg,SCCP} = h\left(\frac{1}{M} \sum_{i=0}^{M-1} \frac{1}{1 + \gamma |P_i|^2} \right) \tag{4.43}$$

To compare the conventional OFDM system with precoded OFDM system we will compare the BER results. And we will do this by using the convexity property of function *h*. The convexity analysis of *h* function from [18] is given in Appendix C. From the analysis, it is seen that the *h* function is convex in all of the SNR regions. This convexity shows us the precoded OFDM system always has better performance than the uncoded case when the receiver is MMSE.

In this chapter we have given the analytical calculations for two different communication systems. In these systems MMSE and ZF receivers are used. In both systems two different cases are investigated. The identity matrix and the DFT matrix are used as precoders in these cases. We have made the SNR and BER calculations and compared the MMSE and ZF receiver by these results. Using the SNR-BER relations it has seen that precoding is effective for ZF receiver only in high SNR regions. In low SNR regions precoding does not bring additional gain in ZF receiver, in fact in these regions identity matrix is more effective. On the contrary in MMSE receiver, precoding is effective in all of the SNR regions, namely using a precoder matrix different from identity matrix always efficient. In order to further illustrate these results we present the simulations in Chapter 5.

CHAPTER 5

NUMERICAL RESULTS

In this section we present the simulation results in order to understand the effects of different precoder matrices and different receiver structures. In simulations the channel is the Rayleigh fading channel. Due to FFT-IFFT computations and cyclic-prefix insertion in OFDM, we simulate the channel as a set of parallel channels represented by a diagonal matrix. The information symbols are BPSK modulated to yield $\{\pm 1\}$. The number of subchannels is M and in simulation $M = \{2,4,8\}$ are used. We use M by M identity, Hadamard and DFT matrices as precoders and ML, MMSE and ZF receivers as decoders.

We have divided simulation into 4 parts. In the first part we compare the BER comparisons for identity, Hadamard, and DFT precoders. In these simulations M=8 is used for ZF and MMSE systems. In the second part BER performances of ML, MMSE and ZF detectors are compared for the precoded system. In this part DFT is used as precoder and the number of subchannels is 8. In the third part, we make simulations to see the effect of number of subchannels. We use $M = \{2,4,8\}$ subchannels for all of the receiver structures and use DFT matrix. At the end we make the rate comparisons for different matrices for MMSE and ZF receivers. In this part we use 8 subchannels and send 1 symbol from this 8 subchannel by spreading it by precoding, then 2, 3…8 symbols are spread over 8 subchannels and compared.

1-Comparison of Different Precoding Matrices

In Figure 5.1, different precoders are compared when MMSE receivers are used. And in Figure 5.2 same comparisons made for ZF receiver. In these simulations number of subchannels is 8. From these simulations we can see that precoding scheme decreases the BER. From analytical results we know that

MMSE gives better result in all the SNR regions and we can verify this claim from Figure 5.1. And from Figure 5.1 we can also
see that the best performance is provided by the DFT matrix. We use this matrix in our remaining simulations to reach the best performance.

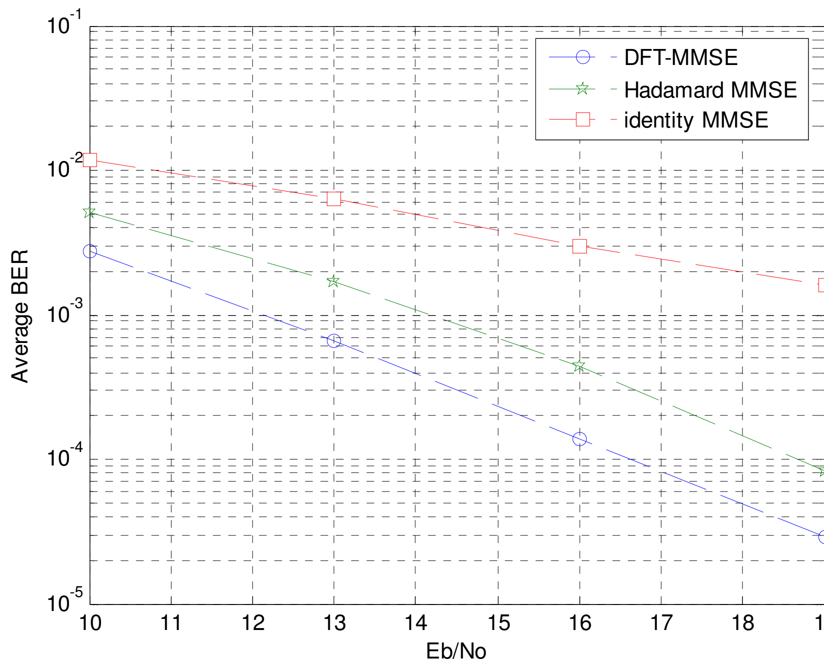

Figure 5.1 Comparisons of different precoders for MMSE receiver

According to the analytical results in the previous chapters it is seen that the precoded system with MMSE receiver has a better performance in all SNR regions than ZF receiver. In ZF receiver, in some SNR regions the BER of the conventional OFDM system is lower than the BER of the precoded system. This result can be seen in Figure 5.2. In low SNR regions using precoder is not effective for ZF receiver.

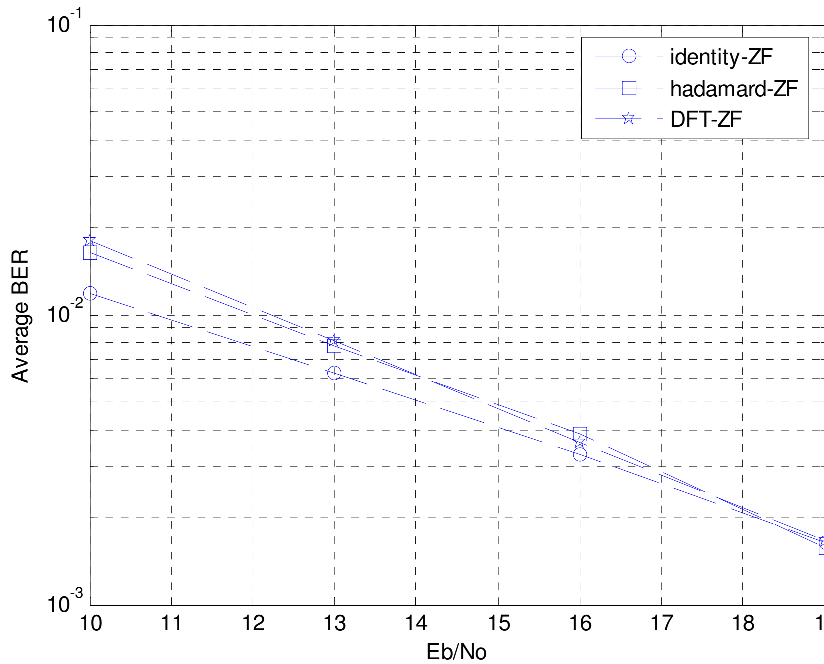

Figure 5.2 Comparison of different precoders for ZF receiver

2-Comparisons of Different Receivers

The precoding with ML receivers is expected to have much better performance than ZF and MMSE receiver. In Figure 5.3 MMSE, ML and ZF decoder performance comparisons are given for precoded system in fading channels. In this case the precoder matrix is used as DFT matrix. Similar results are obtained for other precoding matrices. In all of the cases ML receiver gives the best performance. And from the simulations we can see that MMSE receiver gives better results than ZF receiver as expected.

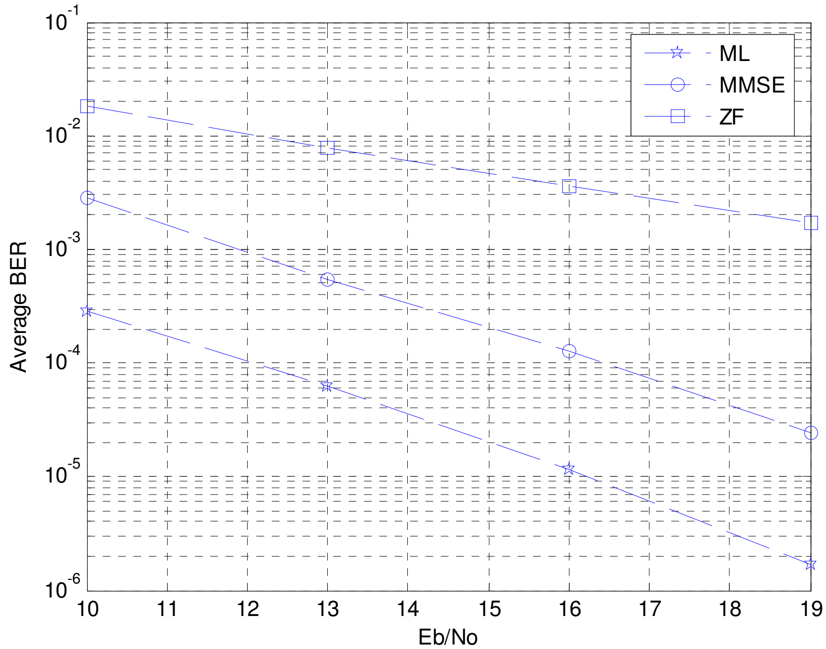

Figure 5.3 Performances comparison for ZF, MMSE and ML receivers with DFT precoder in fading channel

3-Comparisons related to number of parallel channels

When we use the same decoder but we change the dimension of the precoder matrix, the BER performances changes. Increasing the precoder dimension increases the BER performance in fading channels when the decoders are ML or MMSE. This can be seen in Figure 5.4, Figure 5.5 and Figure 5.6. It should be noted that increasing the precoding matrix dimensions brings very high computation load on ML receiver (grows exponentially with the number of channels).

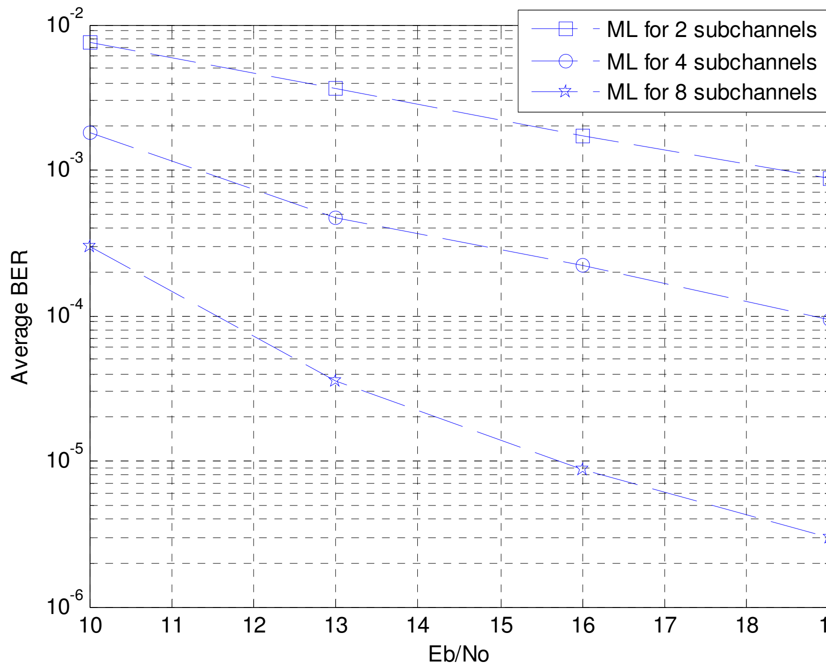

Figure 5.4 ML receiver performance with DFT precoder in fading channel for 2,4 and 8 subchannels

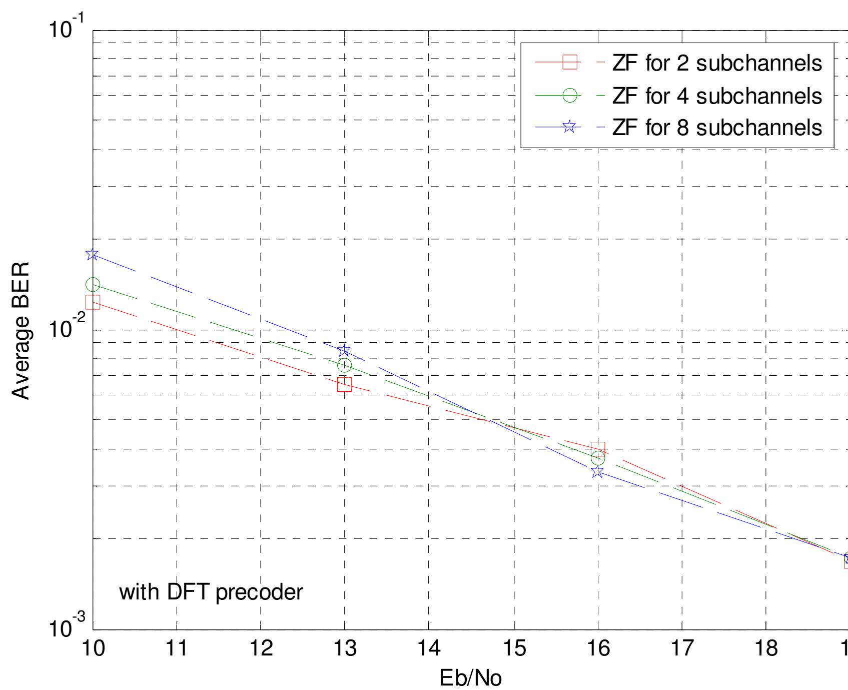

Figure 5.5 ZF receiver performance with DFT precoder in fading channel for 2, 4 and 8 subchannels

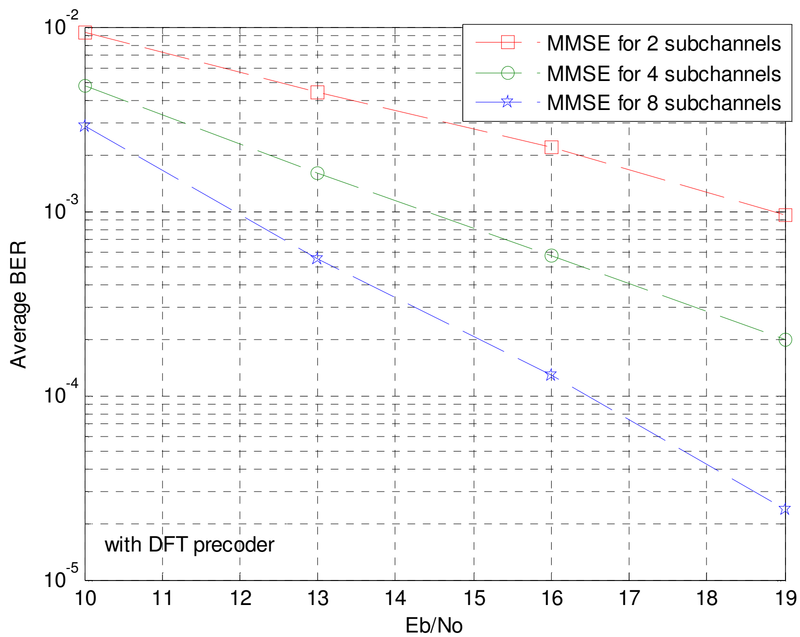

Figure 5.6 MMSE receiver performance with DFT precoder in fading channel for 2, 4 and 8 subchannels

In Figure 5.7 we compare the performance gain of precoding when ML receivers are used. Note that the uncoded system (identity precoder) corresponds to uncoded OFDM system performance. It is clear that there is a significant gain ove uncoded OFDM.

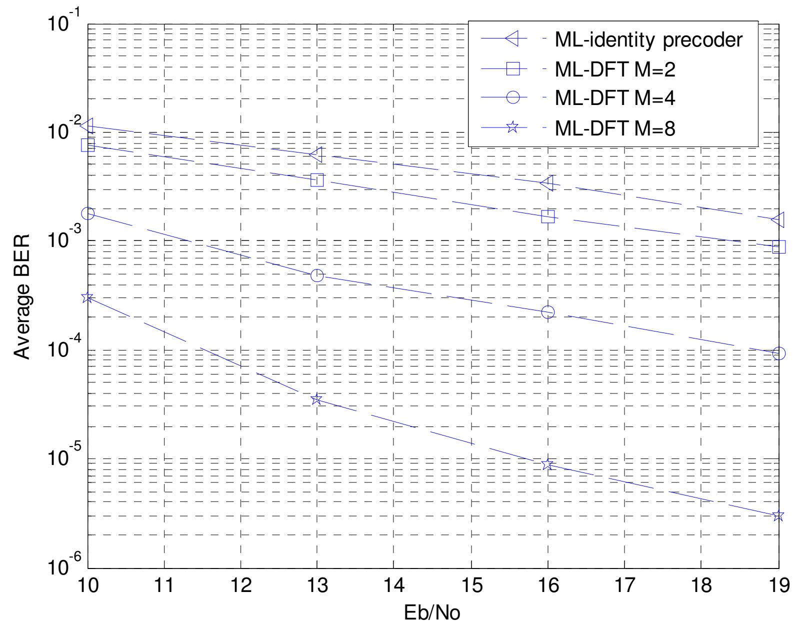

Figure 5.7 ML receiver performance with and without precoder for 2,4,8 channels

4-Performance on AWGN channel

From the simulation results we have seen that the precoder gives better BER results in fading channels. We have repeated the same simulations over an AWGN channel and use DFT matrix as precoder. From Figure 5.8 it can be seen that the DFT and identity matrices gives the same performances. Precoding does not make any performance improvement in AWGN channels, as expected. (As explained in previous chapters, precoders does not enlarge the distance between transmit symbols in the constellation. Therefore when constellation is not sheared by fading, there is no gain that can be realized by precoding.)

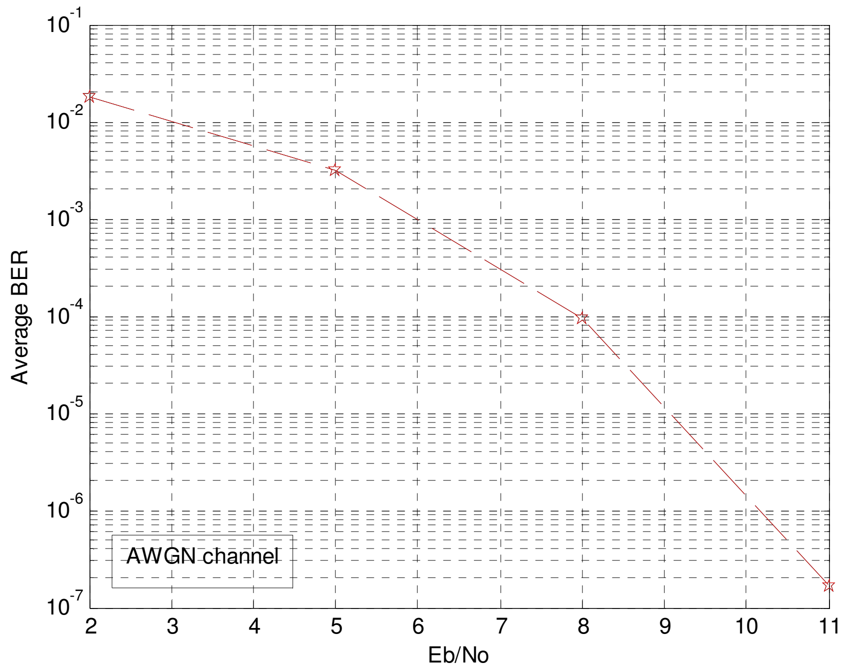

Figure 5.8 ML-MMSE-ZF receiver performances of precoded and uncoded system in AWGN channel

5-Redundant Precoding Comparisons

Finally we make the simulations to illustrate rate-reliability trade-off. In this part 8x8 DFT matrix is used as precoder. At first, 1 symbol is send through 8 subchannels. In other words the same symbol is repeated over 8 parallel channels, we call the transmission rate of such a system as 1/8 symbols per channels.

The rate of 2/8 corresponds to transmission of 2 symbols over 8 parallel channels:

$$\boldsymbol{s} = \boldsymbol{u_1} b_1 + \boldsymbol{u_2} b_2 \tag{5.1}$$

Here the transmit vector $\boldsymbol{s}$ is a linear combination of two vectors $\boldsymbol{u_1}$ and $\boldsymbol{u_2}$; the received vector is,

$$\boldsymbol{r} = \Lambda \boldsymbol{s} + \boldsymbol{w} \tag{5.2}$$

where Λ is the diagonal matrix, as before.

In the following simulations, we use columns of 8x8 DFT matrix which are called as $\boldsymbol{u}_1, \boldsymbol{u}_2, \ldots\ldots, \boldsymbol{u}_k$ as precoding vectors.

From the Figures 5.9 and 5.10 we can see that decreasing rate, i.e. increasing diversity order provides more reliable communication.

With precoding, two important results can be achieved about rate. In ZF receiver it is clearly seen from figures that 8/8 system has a diversity order of 1. Hence every doubling of SNR (3 dB increase) results in 2 fold reduction in BER. (At high SNR $P_e \approx \frac{1}{SNR}$). The 7/8 system has a diversity order of 2. Hence every 3 dB increase in SNR, results in 4 fold reduction in BER, (At high SNR $P_e \approx \frac{1}{SNR^2}$) As expected, 1/8 system has the diversity order of 8, since it is equivalent to repetition coding over 8 parallel channels.

Diversity order for MMSE receiver cannot determined as simply as ZF receiver. We are currently unable to analytically find the diversity order of MMSE receivers. Using the fact that MMSE convergence to ZF receivers at sufficiently high SNR; it can be argued that the diversity order of MMSE system is equal to ZF system at high SNR. But this claim cannot be verified from Figure 5.10. In Figure 5.10 $\frac{E_b}{N_0}$ range is between 10-19 dB. Higher $\frac{E_b}{N_0}$ values may be required to verify this claim.

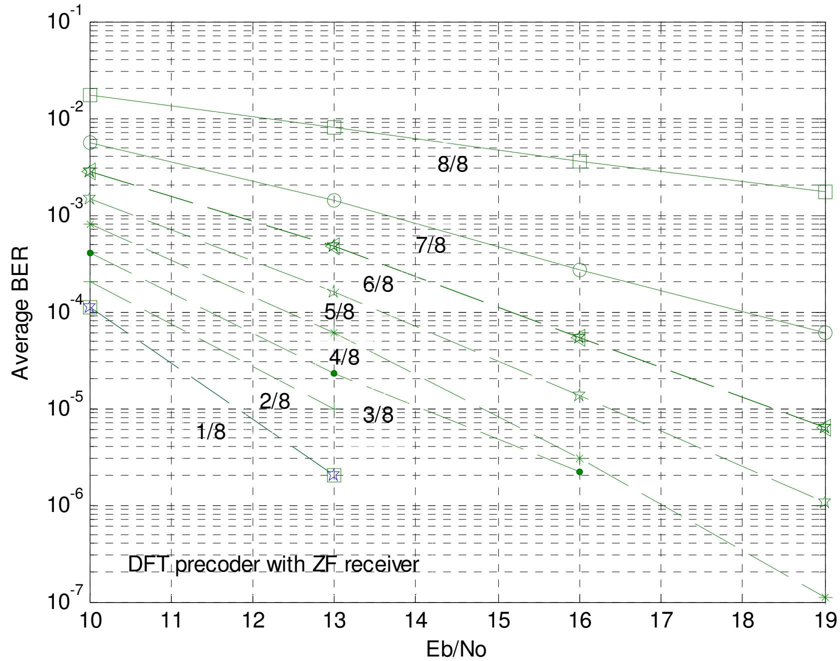

Figure 5.9 Rate comparisons for ZF receiver with DFT precoder

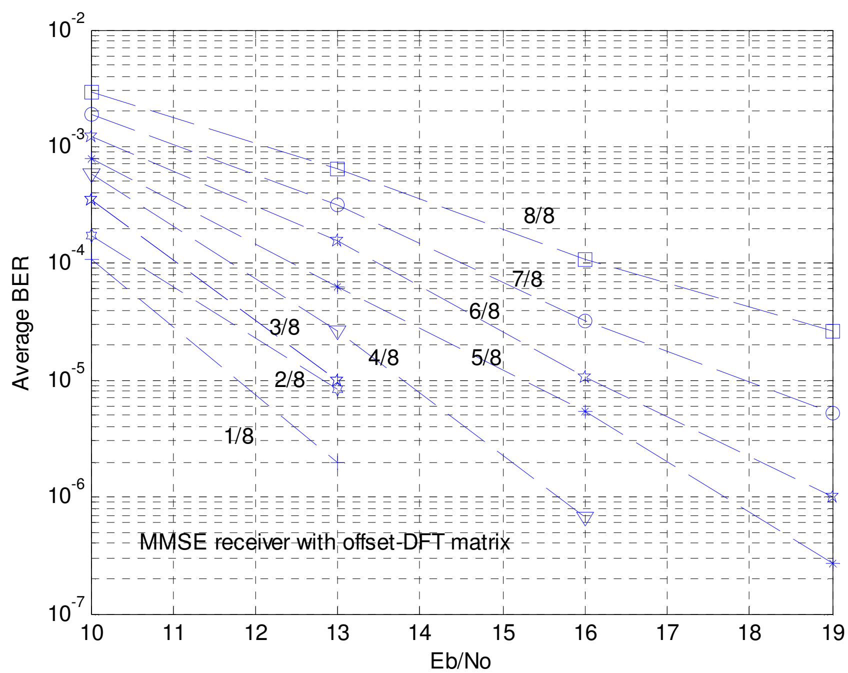

Figure 5.10 Rate comparisons for MMSE receiver with DFT precoder

6-SINR Distribution for Redundant Precoding Systems with MMSE Receivers

In Figure 5.11, the distribution of SINR at different rate values ranging from 1/M to M/M is shown. For this simulation, we have calculated the SINR after MMSE estimation (MMSE receiver) for a system operating at the rate K/M. Y-axis of Figure 5.11 corresponds to distribution of SINR values when system operates at different rates. This graph explains that mean(SINR) after MMSE estimation depreciates from 25 dB (316 in linear scale) to 18 dB (65 in linear scale) as rate increases from 1/256 (repetition coding) to 256/256 (rateless operation).

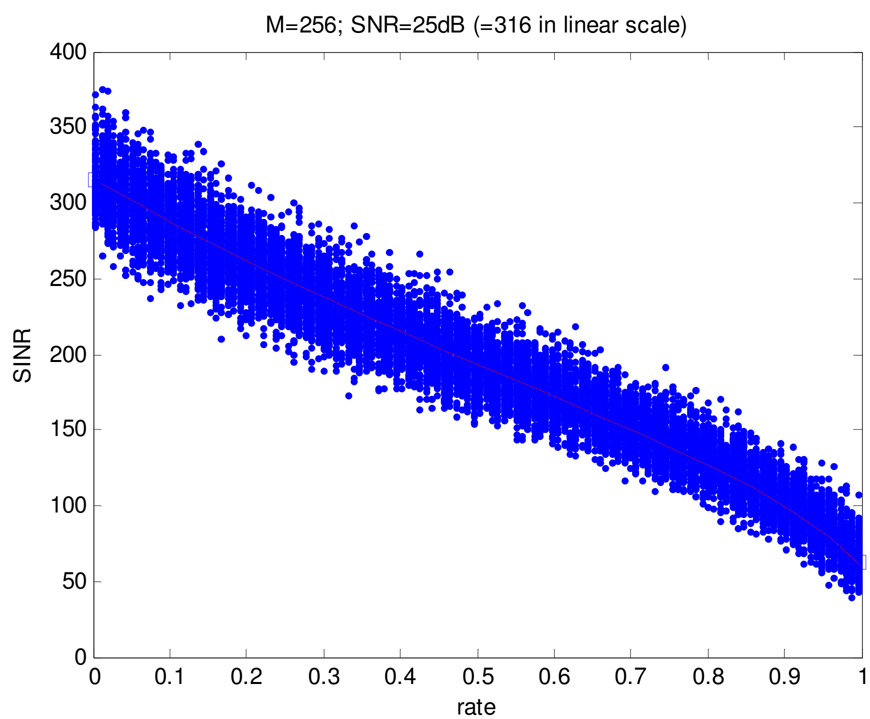

Figure 5.11 SINR distribution graph for different data rates

7-Sensitivity of MMSE Receiver to the Channel Estimation Errors

Up to now, we have assumed that the channel information is perfectly known at the receiver. Here we change this assumption and assume that the channel knowledge is not perfectly known at the receiver and an estimation error exists on the channel gains.

In the following simulation, the precoder performance when CSI is not perfectly accurate is investigated. For this simulation 8x8 DFT precoder matrix is used. The Rayleigh channel coefficients are independently generated as before and MMSE receiver is used. Here we assume that channel gains have some AWGN estimation error, that is:

$$\widetilde{\alpha}_k = \alpha_k + n_{\alpha_k}$$

where α_k is true channel gain and n_{α_k} is complex Gaussian noise with a given variance. Then the MMSE receiver with noisy $\widetilde{\alpha}_k$'s becomes;

$$\boldsymbol{S}_{MMSE} = \widetilde{\boldsymbol{H}}^H \left(\widetilde{\boldsymbol{H}} \widetilde{\boldsymbol{H}}^H + \boldsymbol{N_0 I} \right)^{-1}$$

where $\widetilde{\boldsymbol{H}} = diag\left(\widetilde{\alpha}_1, \widetilde{\alpha}_2, \ldots, \widetilde{\alpha}_{M-1}\right) \boldsymbol{U}$, $\boldsymbol{U}$ is the precoder matrix.

The channel estimation quality is denoted by channel estimation SNR. The Channel estimation SNR defined as:

$$SNR_{ch-est} = \frac{E\{\alpha^2\}}{E\left\{n_{\alpha}^2\right\}} = \frac{1}{E\left\{n_{\alpha}^2\right\}}$$

Here we vary the channel estimation SNR (SNR_{ch-est}) and examine the performance degradation. The results are shown in Figure 5.12.

In Figure 5.13 we examine the performance of ML receiver under the same assumption. We vary channel estimation SNR as in the previous simulation.

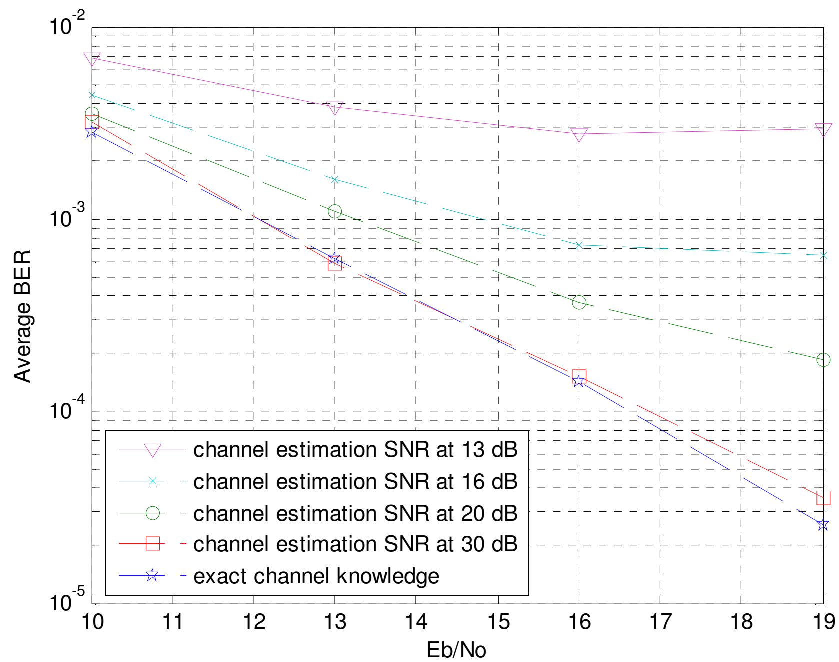

Figure 5.12 Sensitivity of channel information on precoded MMSE receiver performance

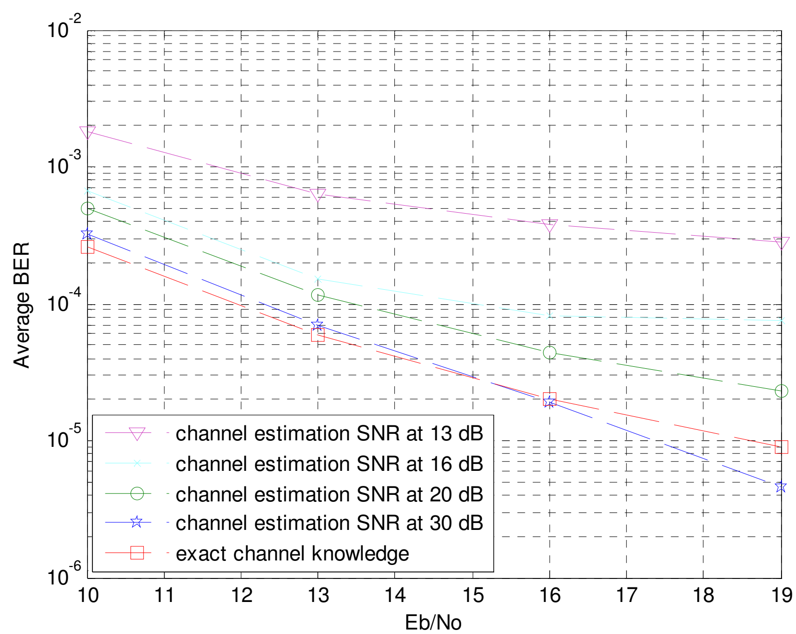

Figure 5.13 Sensitivity of channel information on precoded ML receiver performance

As a conclusion we can say that decreasing the channel estimation SNR decreases the precoded system performance. ML receiver has less sensitivity on quality of channel information relative to the MMSE receiver.

8-Sensitivity of MMSE Receiver to the N_0 Estimation Error

In the next simulation we assume that N_0 which is the addition noise of the receiver is not perfectly known. We assume N_0 estimation has some estimation errors. We investigate the effect of N_0 estimation error on the precoder performance. In this simulation, we use 8x8 DFT matrix as precoder and the following MMSE receiver.

$$\boldsymbol{S}_{MMSE} = \boldsymbol{H}^H \left(\boldsymbol{H}\boldsymbol{H}^H + \widetilde{N_0}\boldsymbol{I} \right)^{-1}$$

Here we take $\widetilde{N_0}$ as 2,4,10 times of then the true N_0 value. Figure 5.13 shows the performance of 8x8 DFT precoder over MMSE receiver when N_0 is not perfectly known.

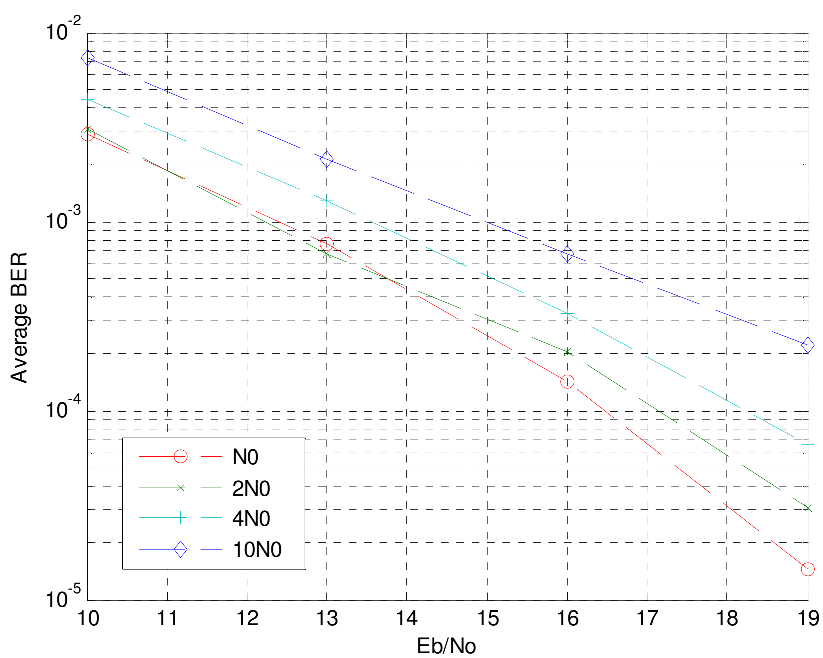

Figure 5.14 Sensitivity of estimation errors on precoded MMSE receiver performance

From Figure 5.14, estimation error on N_0 decreases the system performance. We can say from the simulations that, sensitivity of N_0 estimation errors is not as effective as the sensitivity of channel estimation errors.

9-Comparison of BCH coded OFDM system with precoded MMSE decoded systems

In previous simulations we compare the BER performance of the precoding technique with the uncoded OFDM system. OFDM systems are typically used with error correction coding to improve the BER performance. In this simulation we compared the uncoded OFDM system with precoded and BCH coded OFDM system.

In Figure 5.15, we illustrate BER performance of uncoded OFDM, precoded OFDM with DFT precoding and coded OFDM with BCH coding. The BCH coding system parameters are (n,k)=(15,11). The (15,11) BCH code can correct only one error and has minimum Hamming distance of 3. Here we use a hard decision based error decoding algorithm (conventional BCH decoders) and show the resultant BER.

The BER and diversity can be improved when a soft decision algorithm is used. By design, hard decision algorithms are used for AWGN channels, therefore there can be a large performance gap between a hard decision and soft decision based error correction systems for fading channels.

In Figure 5.15 we present the performance comparison to illustrate the gap between proposed techniques and a *conventional* error correction system.

In Figure 5.16 we make the same comparisons for BCH coded OFDM with a rate of 7/15 and the DFT precoded OFDM with a rate of 4/8 with MMSE receiver. Here BCH coding parameters are (n,k)=(15,7). The (15,7) BCH code can correct 2 errors and has a minimum Hamming distance of 5.

When Figure 5.15 and 5.16 are compared, we see that (15,7) system has much better performance than the (15,11) system. This can be explained by the diversity order of each system which is 1 for (15,11) and 2 for (15,7). Therefore at high SNR, diversity order significantly affects the overall BER performance as has been claimed in Section 2.2. The diversity of MMSE receiver in Figure 5.15 is 3 at high SNR (since MMSE approaches ZF, and ZF plots are given in Figure 5.9) and 5 at high SNR for Figure 5.16.

As a conclusion, we can say that precoding with DFT matrix can have a better BER performance in comparison with the conventional hard decision based error correction techniques. A valuable future work can be a similar comparison with the soft decision based decoders.

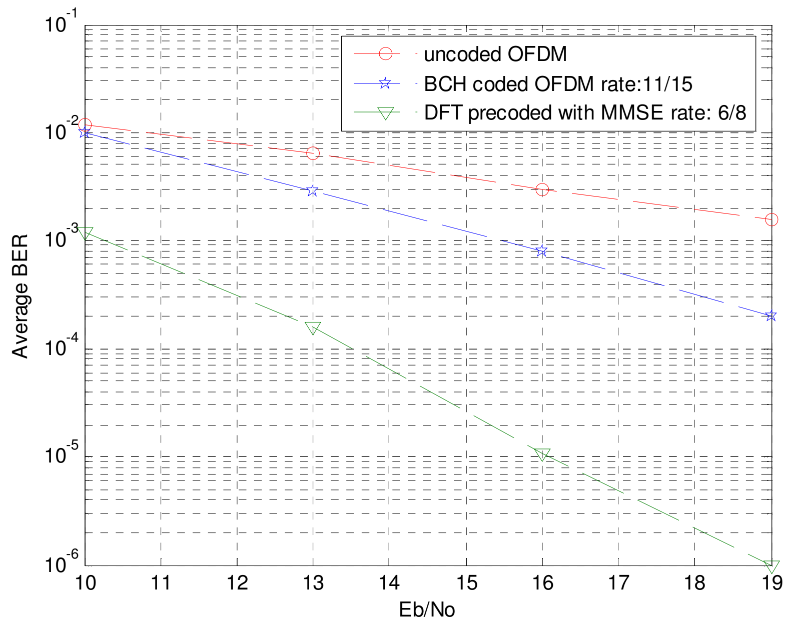

Figurte 5.15 Comparison for precoded OFDM and BCH coded OFDM with rate of 11/15

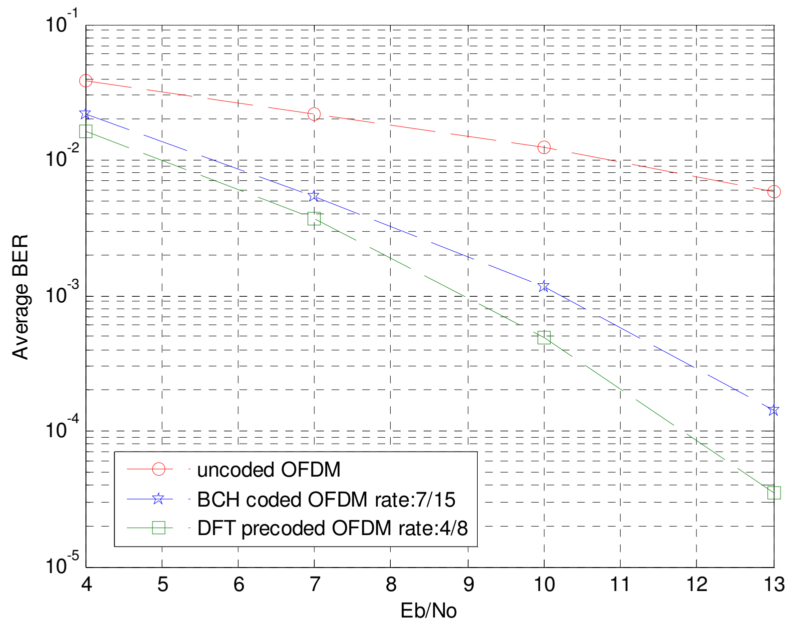

Figure 5.16 Comparison for precoded OFDM and BCH coded OFDM with rate of 7/15

CHAPTER 6

CONCLUSION

In this thesis we have investigated communication over fading channels. Achieving reliable communication over these types of channels is difficult because of the multipath fading problem. Diversity concept is a way to overcome such problems.

Typically diversity is achieved at the cost of transmission rate. In other words the symbol should be repeated over independently fading channels K times to achieve K fold diversity. Repetition of the symbol is the simplest method to achieve diversity.

Precoding is a relatively novel idea to achieve diversity. As discussed in Chapter 2, precoding can be equivalently considered as constellation rotation. The constellation rotation brings diversity gain without reducing rate or increasing power. Hence it can be applied without any harm to system resources.

In this thesis, we have studied different receiver structures to realize diversity gain by precoding. Here, we examined the gap between MMSE, ZF receivers and ML receiver. It has been noted MMSE receiver provides significant gain over uncoded system (without precoding). But the performance gain is still at a significant disadvantage in comparison to ML receiver.

We have studied the case when rate is allowed to be reduced so that K/M symbols are transmitted per parallel channel instead of M/M symbols. The MMSE and ZF receiver performances at K/M rate are studied using computer simulations.

The sensitivity of channel information and the sensitivity of N_0 estimation errors when MMSE and ML receiver are used are considered. When ML receiver is used channel estimation quality is not as critical as it is in MMSE receiver.

The coded OFDM system with BCH coding is compared with precoded OFDM MMSE decoded system. From simulation results it is seen that precoding with DFT matrix can have a better BER performance in comparison with the *conventional hard decision based error correction techniques*. A valuable future work can be a similar comparison with the soft decision based decoders.

There is a large gap between the BER performances of ML receiver and MMSE receiver. Using MMSE receiver is simpler than ML receiver but the performance gap between two receivers cannot be neglected. To reach ML performance at reduced computation complexity is an important research goal. The performance gap can be recovered by iterative decoders. Iterative decoders to reach ML performance by MMSE receiver complexity constitutes future research for rotational coding technique.

REFERENCES

[1] W. Zou and Y.Wu, COFDM an Overview, IEEE Transactions on Broadcasting, Volume 41, Issue 1, Pages:1-8,, March 1995

[2] Z. Wang and G.B. Giannakis, Complex-Field Coding For OFDM over Fading Wireless Channels, IEEE Transactions on Information Theory, Volume 49, Issue 3, Pages:707-720, March 2003

[3] D. Rainish, Diversity Transform for Fading Channels, IEEE Transactions on Communications, Volume 44, Issue 12, Pages: 1653-1661, December 1996

[4] C. Lamy, J. Boutros, On random rotations diversity and minimum MSE decoding of lattices, IEEE Transactions on Information Theory, Volume 46, Issue 4, Pages: 1584-1589, July 2000

[5] Su Borching, R.P. Vaidyanathan, Distributed antipodal paraunitary precoders for OFDM systems, IEEE Pacific Rim Conference on Communications, Computers and signal Processing, 2005. PACRIM. 2005, Pages: 193- 196 , 24-26 Aug. 2005

[6] See-May Phoong, Kai-Yen Chang, Yuan-Pei Lin, Antipodal paraunitary precoding for OFDM application, International Symposium on Circuits and Systems, 2004. ISCAS '04. Proceedings of the 2004, Volume: 5, Page: V-425- V-428 , 23-26 May 2004

[7] S.M. Phoong, Kai-Yen Chang, Antipodal paraunitary matrices and their application to OFDM systems, IEEE Transactions on Signal Processing, Volume 53, Issue 4, Pages: 1374-1386, April 2005

[8] Zhengdao Wang, G.B. Giannakis, Linearly precoded or coded OFDM against wireless channel fades? , 2001 IEEE Third Workshop on Signal Processing Advances in Wireless Communications, 2001. (SPAWC '01), Pages: 267-270, 2001

[9] Yuan-Pei Lin, See-May Phoong , BER optimized channel independent precoder for OFDM system, Global Telecommunications Conference. GLOBECOM '02. IEEE, 2002

[10] Richard D.J Van Nee, OFDM for Wireless Multimedia Communications, Artech House, 2000

[11] Yanwu Ding, T.N Davidson, Zhi-Quan Luo, Kon Max Wong, Minimum BER block precoders for zero-forcing equalization, IEEE Transactions on Signal Processing, Volume 51, Issue 9, Pages: 2410-2423, September 2003

[12] M. Debbah, P. Loubaton, M. de Courville, Asymptotic performance of successive interference cancellation in the context of linear precoded OFDM systems, IEEE Transactions on Communications, Volume 52, Issue 9, Pages:1444-1448, September 2004

[13] S. Tamura, M.Fujii, M. Itami, K. Itoh, An iterative detection of precoded OFDM under frequency selective fading channels, IEEE 16th International Symposium on Personal, Indoor and Mobile Radio Communications, 2005. PIMRC 2005, 11-14, Volume 4, Pages: 2489- 2494 Vol. 4, Sept. 2005

[14] P.-J. Bouvet, M. Helard, V. Le Nir, Low complexity iterative receiver for linear precoded OFDM, IEEE International Conference on Wireless And Mobile Computing, Networking And Communications, 2005. (WiMobapos;2005), Volume 1, Pages: 50 - 54 Vol. 1, 22-24 Aug. 2005

[15] L. Rugini, P. Banelli, G.B. Giannakis, MMSE-based local ML detection of linearly precoded OFDM signals, IEEE International Conference on Communications, 2004 , Volume 6, Pages : 3270 - 3275 Vol.6, 20-24 June 2004

[16] David Tse, Pramod Viswanath, Fundamentals of Wireless Communication, Cambridge University Press, 2005

[17] Zhengdao Wang, G.B Giannakis, Complex-field coding for OFDM over fading wireless channels, IEEE Transactions on Information Theory, Volume 49, Issue 3, Pages: 707 – 720, March 2003

[18] Yuan-Pei Lin, See-May Phoong, BER minimized OFDM systems with channel independent precoders, IEEE Transactions on Signal Processing, Volume 51, Issue 9, Pages: 2369 – 2380, Sept. 2003

APPENDIX A

PERFORMANCE MEASUREMENTS IN FADING CHANNELS

In frequency fading channels the fading coefficients are random, so the measurements of the performance of the system are also random. To characterize the system performance in such case, the pdf of the measurement should be obtained. But characterizing the system with whole pdf is not practical. One of the most common ways of characterizing is doing the measurement with the average value. In such case the average bit error rate (BER) is a useful measure. We now describe the three common measures of the performance of a communication system: Mean Square Error (MSE), Signal to Noise Ratio (SNR) and Bit Error Rate (BER).

A.1- MSE

The Mean Square Error (MSE) is estimation $\hat{x}$ of the transmitted symbol x.

$$MSE = E\left\{|\hat{x} - x|^2\right\} \qquad 0 < MSE < 1 \tag{A.1}$$

The smaller the MSE, the better the system since the estimation matches more closely to the desired value.

A.2-SNR

Signal to noise ratio is the ratio between the signal energy and the noise energy. The general definition of signal to noise ratio is,

$$SNR = \frac{average\ received\ signal\ energy\ per\ symbol\ time}{noise\ energy\ per\ symbol\ time} \tag{A.2}$$

Consider the received vector in a system,

$$\boldsymbol{y} = \boldsymbol{Hx} + \boldsymbol{n} \tag{A.3}$$

In this system noise energy per symbol time is N_0 and signal energy is a^2

$$SNR = \frac{a^2}{N_0} \qquad 0 < SNR < \infty \tag{A.4}$$

The higher the SNR the better the system, since the desired component signal energy is higher than the undesired component noise energy.

A.3- BER

The performance of a digital communication system is given in terms of symbol error probability or bit error probability. The bit error rate is defined as the bit error probability. If the noise component of a system is Gaussian distributed the symbol error probability P_e can be expressed as a function of SNR,

$$P_e = \alpha Q\left(\sqrt{\beta SNR}\right) \tag{A.5}$$

α and β are the constants that depend on the signal constellation. $BER \approx \frac{P_e}{k}$ $k = \log_2 M$ is the number of bits per symbol and M is the constellation size. The lower the BER the better the system, since it means that less error is made when estimating the transmitted bits.

APPENDIX B

MAXIMUM SINR AND MINIMUM MMSE FILTERS

We examine the relation between max SINR and min MMSE filters in this section. Assume that signal of interest is captured by a noisy receiver according to the following model:

$$\boldsymbol{r} = \boldsymbol{u_0} x + \boldsymbol{n} \tag{B.1}$$

Here, x is the scalar that we would like to estimate. It is known that $E\{x\} = 0$, $E\left\{x^2\right\} = \sigma_x^2$. $\boldsymbol{r}$ is Nx1 column vector (receive vector). $\boldsymbol{u_0}$ is modulating vector for scalar x. $\boldsymbol{n}$ is Nx1 vector representing noise with auto-correlation matrix $\boldsymbol{R_n}$.

Max SINR with linear combining

Assume an estimate for x is formed as follows,

$$\hat{x} = \boldsymbol{w^H} \boldsymbol{r} \tag{B.2}$$

$\boldsymbol{w}$ is the combining vector to be determined. Then,

$$\hat{x} = \left(\boldsymbol{u^H} \boldsymbol{u_0}\right) x + \boldsymbol{w^H} \boldsymbol{n} = \alpha x + \beta \tag{B.3}$$

$$(SINR)_{after} = \frac{E\left\{(\alpha x)^2\right\}}{E\left\{\beta^2\right\}}$$

$$= \sigma_x^2 \frac{\left(\boldsymbol{w^H} \boldsymbol{u_0} \boldsymbol{u_0^H} \boldsymbol{w}\right)}{\left(\boldsymbol{w^H} \boldsymbol{R_n} \boldsymbol{w}\right)} \tag{B.4}$$

we would like to maximize $(SINR)_{after}$ by proper selection of $\boldsymbol{w}$.

$$\max_{\boldsymbol{w}}(SINR)_{after} = \max_{\boldsymbol{w}} \frac{\|\boldsymbol{w}^H \boldsymbol{u}_0\|^2}{\boldsymbol{w}^H \boldsymbol{R}_n \boldsymbol{w}}$$

$$= \max_{\boldsymbol{w}_d} \frac{\|\left(\boldsymbol{R}_n^{-\frac{1}{2}} \boldsymbol{w}_d\right)^H \boldsymbol{u}_0\|^2}{\left(\boldsymbol{R}_n^{-\frac{1}{2}} \boldsymbol{w}_d\right)^H \boldsymbol{R}_n \left(\boldsymbol{R}_n^{-\frac{1}{2}} \boldsymbol{w}_d\right)} \tag{B.5}$$

Maximizing with respect to $\boldsymbol{w}_d$ leads to

$$\max_{w_d} = \frac{\|\boldsymbol{w}_d^H \boldsymbol{R}_n^{-\frac{1}{2}} \boldsymbol{u}_0\|^2}{\boldsymbol{w}_d^H \boldsymbol{w}_d}$$

that is when $\boldsymbol{w}_d = \boldsymbol{R}_n^{-\frac{1}{2}} \boldsymbol{u}_0$, then the optimal weight vector becomes

$$\boldsymbol{w}_{d_{opt}} = \boldsymbol{R}_n^{-\frac{1}{2}} \boldsymbol{w}_d$$

and

$$\boldsymbol{w}_{opt} = \boldsymbol{R}_n^{-1} \boldsymbol{u}_0 \tag{B.6}$$

This is another illustration of the optimality of whitened match filter for SINR maximization.

The max SINR after combining is then;

$$\max(SINR)_{after} = \frac{\sigma_x^2 \boldsymbol{w}^H \boldsymbol{u}_0 \boldsymbol{u}_0^H \boldsymbol{w}}{\boldsymbol{w}^H \boldsymbol{R}_n \boldsymbol{w}} \Big|_{\boldsymbol{w} = \boldsymbol{w}_{opt} = \boldsymbol{R}_n^{-1} \boldsymbol{u}_0}$$

$$=\sigma_x^2 \frac{\left(\boldsymbol{u}_0^H \boldsymbol{R}_n^{-1} \boldsymbol{u}_0\right)\left(\boldsymbol{u}_0^H \boldsymbol{R}_n^{-1} \boldsymbol{u}_o\right)}{\boldsymbol{u}_0^H \boldsymbol{R}_n^{-1} \boldsymbol{R}_n \boldsymbol{R}_n^{-1} \boldsymbol{u}_o}$$

$$=\sigma_x^2 \boldsymbol{u}_0^H \boldsymbol{R}_n^{-1} \boldsymbol{u}_0 \qquad \text{(B.7)}$$

min MMSE filter

Here, we would like to estimate $\boldsymbol{x}$ according to

$$\hat{x} = \boldsymbol{w}^H \boldsymbol{r} \qquad \text{(B.8)}$$

This time, we would like to form the weights such that $E\left\{|x-\hat{x}|^2\right\}$ is minimized.

$$J = E\left\{|x-\hat{x}|^2\right\} \qquad \text{(B.9)}$$

$$\Delta_{w*} J = E\left\{-2\left(x-\hat{x}\right)\boldsymbol{r}\right\} = 0$$

$$= E\left\{x\boldsymbol{r} - \boldsymbol{w}^H \boldsymbol{r}\boldsymbol{r}^H\right\} = 0 \qquad \text{(B.10)}$$

then $\boldsymbol{R}_r \boldsymbol{w} = \boldsymbol{r}_{xr}$, $\boldsymbol{w}_{opt} = \boldsymbol{R}_r^{-1} \boldsymbol{r}_{xr}$, Where $\boldsymbol{R}_r = E\left\{\boldsymbol{r}\boldsymbol{r}^H\right\}$ and $\boldsymbol{r}_{xr} = E\left\{x\boldsymbol{r}\right\}$. The value for minimum MSE can be calculated as follows:

$$J_{\min} = E\left\{\left(x-\hat{x}\right)^2\right\}\Big|_{\hat{x}=\boldsymbol{w}_{opt}^H \boldsymbol{r}}$$

$$= E\left\{\left(x-\hat{x}\right)\left(x-\boldsymbol{w}_{opt}^H \boldsymbol{r}\right)\right\}$$

$$= E\left\{\left(x-\hat{x}^H\right)x\right\}$$

$$= E\left\{x^2-\left(\boldsymbol{w}_{opt}^H \boldsymbol{r}\right)x\right\}$$

$$= \sigma_x^2 - \boldsymbol{w}_{opt}^H \, \boldsymbol{r}_{xr}$$

$$J_{\min} = \sigma_x^2 - \mathbf{r}_{\mathbf{xr}}^{\mathbf{H}} \, \boldsymbol{R}_r^{-1} \, \boldsymbol{r}_{xr} \tag{B.11}$$

Connection between min MMSE $\left(J_{\min}\right)$ and max SINR $\max(SINR)_{after}$

In this section, we illustrate the connection between min MMSE $\left(J_{\min}\right)$ value of optimal linear MMSE filter and max SINR filter derived earlier. The observation model for both problem is as follows:

$$\boldsymbol{r} = \boldsymbol{u}_{\mathbf{0}} \, x + \boldsymbol{n} \tag{B.12}$$

for min MMSE filter :

$$\boldsymbol{R}_r = \boldsymbol{u}_{\mathbf{0}} \, \boldsymbol{u}_{\mathbf{0}}^H \, \sigma_x^2 + \boldsymbol{R}_n \tag{B.13}$$

$$\boldsymbol{r}_{xr} = \boldsymbol{u}_{\mathbf{0}} \, \sigma_x^2 \tag{B.14}$$

$$\boldsymbol{w}_{opt} = \boldsymbol{R}_r^{-1} \, \boldsymbol{r}_{xr} \tag{B.15}$$

$$J_{\min} = \sigma_x^2 \left(1 - \boldsymbol{u}_{\mathbf{0}}^H \, \boldsymbol{R}_r^{-1} \, \boldsymbol{u}_{\mathbf{0}} \, \sigma_{\mathbf{x}}^2\right) \tag{B.16}$$

For max SINR filter :

$\boldsymbol{w}_{opt} = \alpha \boldsymbol{R}_n^{-1} \, \boldsymbol{u}_{\mathbf{0}}$ where α is any complex number,

Remember that maxSINR filter produces following SINR:

$$\max(SINR)_{after} = (SINR)_{\max} = \boldsymbol{u}_{\mathbf{0}}^H \, \boldsymbol{R}_n^{-1} \, \boldsymbol{u}_{\mathbf{0}} \tag{B.17}$$

To connect $J_{\min}$ value to the $(SINR)_{\max}$ value, we calculate $\boldsymbol{R}_r^{-1}$ using matrix inversion lemma *, as follows:

---

*Matrix Inversion Lemma: $\mathbf{(A+BCD)^{-1}=A^{-1}-A^{-1}B(C^{-1}+DA^{-1}B)^{-1}DA^{-1}}$

$$\boldsymbol{R}_r^{-1} = \left(\boldsymbol{R}_n + \sigma_x^2 \boldsymbol{u}_0 \boldsymbol{u}_0^H\right)^{-1}$$

$$= \boldsymbol{R}_n^{-1} - \frac{\boldsymbol{R}_n^{-1} \boldsymbol{u}_0 \boldsymbol{u}_0^H \boldsymbol{R}_n^{-1}}{1 + \sigma_x^2 \boldsymbol{u}_0^H \boldsymbol{R}_n^{-1} \boldsymbol{u}_0} \sigma_x^2 \qquad \text{(B.18)}$$

Inserting $\boldsymbol{R}_r^{-1}$, relation from (B.18) to $\boldsymbol{w}_{opt} = \boldsymbol{R}_r^{-1} \boldsymbol{r}_{xr}$, we get

$$\boldsymbol{w}_{opt} = \left(\boldsymbol{R}_n^{-1} - \frac{\sigma_x^2 \boldsymbol{R}_n^{-1} \boldsymbol{u}_0 \boldsymbol{u}_0^H \boldsymbol{R}_n^{-1}}{1 + \sigma_x^2 \boldsymbol{u}_0^H \boldsymbol{R}_n^{-1} \boldsymbol{u}_0} \right) \boldsymbol{u}_0 \sigma_x^2$$

$$\boldsymbol{w}_{opt} = \boldsymbol{R}_n^{-1} \boldsymbol{u}_0 \left(1 - \frac{\sigma_x^2 \boldsymbol{u}_0^H \boldsymbol{R}_n^{-1} \boldsymbol{u}_0}{1 + \sigma_x^2 \boldsymbol{u}_0^H \boldsymbol{R}_n^{-1} \boldsymbol{u}_0} \right) \sigma_x^2$$

$$= \boldsymbol{R}_n^{-1} \boldsymbol{u}_0 \left(\frac{\sigma_x^2}{1 + \sigma_x^2 \boldsymbol{u}_0^H \boldsymbol{R}_n^{-1} \boldsymbol{u}_0} \right) \qquad \text{(B.19)}$$

By comparing Equation (B.19) with the SINR minimizing filter in (B.6), we see that optimal MSE minimizing filter is the scaled version of max-SINR filter. Therefore MMSE filter also maximizes SINR.

Inserting the equation above into the $J_{\min}$ relation given in (B.16), we get;

$$J_{\min} = \sigma_x^2 \left(1 - \sigma_x^2 \boldsymbol{u}_0^H \boldsymbol{R}_n^{-1} \boldsymbol{u}_0 + \frac{\sigma_x^2 \left(\boldsymbol{u}_0^H \boldsymbol{R}_n^{-1} \boldsymbol{u}_0\right)\left(\boldsymbol{u}_0^H \boldsymbol{R}_n^{-1} \boldsymbol{u}_0\right) \sigma_x^2}{1 + \sigma_x^2 \boldsymbol{u}_0^H \boldsymbol{R}_n^{-1} \boldsymbol{u}_0} \right) \qquad \text{(B.20)}$$

$$= \sigma_x^2 \left[1 - (SINR)_{\max} + \frac{\left[(SINR)_{\max}\right]^2}{1 + (SINR)_{\max}} \right]. \qquad \text{(B.21)}$$

and finally,

$$\frac{J_{\min}}{\sigma_x^2} = \frac{1}{1 + (SINR)_{\max}} \qquad \text{(B.22)}$$

calling $\frac{J_{min}}{\sigma_x^2}$ as normalized MMSE ε_{MMSE}, then the relation is as

$$(SINR)_{max} = \frac{1}{\varepsilon_{MMSE}} - 1 \tag{B.23}$$

SINR-MSE Relation for ZF Receiver

In the previous part we examined the relation between max SINR and min MMSE. In this part we investigate MSE-SNR relations for a ZF receiver. The received vector is as follows:

$$\boldsymbol{r} = \boldsymbol{Hx} + \boldsymbol{n} \tag{B.24}$$

Under ZF receiver operation, the received vector is operated by pseudo inverse of **H** matrix and we get,

$$\hat{\boldsymbol{x}} = \boldsymbol{H}^{+}\boldsymbol{r} \tag{B.25}$$

$\boldsymbol{H}^{+}$ is the pseudo inverse of $\boldsymbol{H}$ for an overdetermined system which is

$$\boldsymbol{H}^{+} = \left(\boldsymbol{H}^{H}\boldsymbol{H}\right)^{-1}\boldsymbol{H}^{H} \tag{B.26}$$

then $\hat{\boldsymbol{x}}$ becomes,

$$\hat{\boldsymbol{x}} = \left(\boldsymbol{H}^{H}\boldsymbol{H}\right)^{-1}\boldsymbol{H}^{H}\boldsymbol{H}x + \left(\boldsymbol{H}^{H}\boldsymbol{H}\right)^{-1}\boldsymbol{H}\boldsymbol{n}$$

$$\hat{\boldsymbol{x}} = \boldsymbol{x} + \underbrace{\left(\mathbf{H}^{\mathbf{H}}\mathbf{H}\right)^{-1}\mathbf{H}\,\mathbf{n}}_{\varepsilon} \tag{B.27}$$

The error covariance matrix for $\varepsilon = \boldsymbol{x} - \hat{\boldsymbol{x}}$ is,

$$\boldsymbol{C}_{\varepsilon} = \boldsymbol{E}\left\{\left(\boldsymbol{x} - \hat{\boldsymbol{x}}\right)\left(\boldsymbol{x} - \hat{\boldsymbol{x}}\right)\right\}$$

$$\boldsymbol{C}_{\varepsilon} = \boldsymbol{E}\{\varepsilon\varepsilon^{\boldsymbol{H}}\}$$

$$= \left(\boldsymbol{H}^{H}\boldsymbol{H}\right)^{-1}\boldsymbol{H}\boldsymbol{R}_{n}\boldsymbol{H}^{H}\left(\boldsymbol{H}^{H}\boldsymbol{H}\right)^{-1} \tag{B.28}$$

When $\boldsymbol{R_n}$ is white noise with variance N_0, $\boldsymbol{R_n} = N_0 \boldsymbol{I}$; we get $\boldsymbol{C}_\varepsilon$ as follows:

$$\boldsymbol{C}_\varepsilon = \left(\boldsymbol{H}^{\boldsymbol{H}} \boldsymbol{H}\right)^{-1} \boldsymbol{N_0} \tag{B.29}$$

Finally we write $\hat{\boldsymbol{x}}$ as,

$$\hat{\boldsymbol{x}} = \boldsymbol{x} + \varepsilon \tag{B.30}$$

where ε is $\mathrm{N}\left(0, \boldsymbol{C}_\varepsilon\right)$.Then the kth component of $\hat{\boldsymbol{x}}$ which is $\left(\hat{\boldsymbol{x}}\right)_k$, becomes

$$\left(\hat{\boldsymbol{x}}\right)_k = (\boldsymbol{x})_k + (\varepsilon)_k \tag{B.31}$$

Then the SINR of $\left(\hat{\boldsymbol{x}}\right)_k$ is,

$$(SINR) = \frac{E\left\{|(\boldsymbol{x})_k|^2\right\}}{\left(\boldsymbol{C}_\varepsilon\right)_{kk}} = \frac{E\left\{|(\boldsymbol{x})_k|^2\right\}}{N_0\left[\left(\boldsymbol{H}^{\boldsymbol{H}} \boldsymbol{H}\right)^{-1}\right]_{kk}} = \frac{E\left\{|(\boldsymbol{x})_k|^2\right\}}{(MSE)_k} \tag{B.32}$$

Where $\left(\boldsymbol{C}_\varepsilon\right)_{kk}$ is (kk)$^{\text{th}}$ entry of $\boldsymbol{C}_\varepsilon$. When $\left(\hat{\boldsymbol{x}}\right)_k$ is of unit variance then the relation between SINR and MSE for ZF receiver is:

$$(SINR)_k = \frac{1}{(MSE)_k} \tag{B.33}$$

APPENDIX C

CONVEXITY ANALYSIS OF MMSE AND ZF RECEIVERS

We present convexity analysis given in [18] for completeness. For understanding
the effect of precoder we will use the relation between MSE and SNR in ZF receivers. This relation is,

$$SNR = \frac{1}{MSE} \tag{C.1}$$

Additional information about SNR-BER relations for ZF and MMSE receivers is given in Appendix B. According to equation (C.1),

$$BER = Q\left(\sqrt{SNR}\right) = Q\left(\frac{1}{\sqrt{MSE}}\right) \tag{C.2}$$

Convexity Analysis of ZF receiver from [19]

To analyze BER performance we can use the function f that is defined as $f(x) = Q\left(\frac{1}{\sqrt{x}}\right)$. Here $f(x)$ corresponds to SNR value and x is MSE value. The BER performance is closely related to the convexity properties of the function f.

$$BER_i = Q\left(\sqrt{\frac{\varepsilon_s}{\sigma^2(i)}}\right) = f\left(\frac{1}{SNR_i}\right) \tag{C.3}$$

A set C is convex if the line segment between any two points in C lies in C, i.e., if for any $x_1, x_2 \in C$ and any θ with$0 \le \theta \le 1$, we have

$$\theta x_1 + (1-\theta)\, x_2 \in C \tag{C.4}$$

Convexity of $f(x)$:

Let $u(x) = \frac{1}{\sqrt{x}}$ $\quad for\ x \geq 0$ then $f(x) = Q\left(u(x)\right)$.

First and second derivatives of $f(x)$ is important for convexity analysis.

$$f'(x) = Q'\left(u(x)\right) u'(x) = \frac{1}{2\sqrt{2\pi}} e^{-\frac{1}{2x}} x^{-\frac{3}{2}}$$

$$f''(x) = Q''\left(u(x)\right)\left[u'(x)\right]^2 + Q'\left(u(x)\right) u''(x) = \frac{1}{4\sqrt{2\pi}} e^{-\frac{1}{2x}} x^{-\frac{7}{2}} (1 - 3x)$$

For $x \leq \frac{1}{3}$, $f''(x) \geq 0$ and $f(x)$ is convex for this region and for $x > \frac{1}{3}$, $f''(x) < 0$ and $f(x)$ is concave for this region. $f\left(\frac{1}{SNR_i}\right)$ is convex for $\frac{1}{SNR_i} \leq \frac{1}{3} \rightarrow SNR_i \geq 3$ the i^th^ subchannel is operating in convex region and $SNR_i \leq Q\left(\sqrt{3}\right) = 0.0416$. $f\left(\frac{1}{SNR_i}\right)$ is concave for $\frac{1}{SNR_i} \geq \frac{1}{3} \rightarrow SNR_i < 3$ the i^th^ subchannel is operating in the concave region and SNR_i >0.0416.

To find which precoder operates in convex region it is necessary to define SNR quantities.

$$\gamma_0 = \min_i \frac{3}{|P_i|^2}, \quad \bar{\gamma} = \frac{1}{M} \sum_{i=0}^{M-1} \frac{3}{|P_i|^2}, \quad \gamma_1 = \max_i \frac{3}{|P_i|^2} \qquad \text{(C.5)}$$

and the SNR regions are:

$$\Re_{low} = \left\{\gamma | \gamma \leq \gamma_0\right\}, \quad \Re_{mid} = \left\{\gamma | \gamma_0 < \gamma < \gamma_1\right\}, \quad \Re_{high} = \left\{\gamma | \gamma_1 \geq \gamma\right\} \qquad \text{(C.6)}$$

First consider the SC-CP system:

When $\gamma = \bar{\gamma}$

$$SNR_{sc-cp,i} = \frac{1}{\frac{1}{M}\sum_{i=0}^{M-1}\frac{1}{\gamma |P_i|^2}} = \frac{1}{\frac{1}{M}\sum_{i=0}^{M-1}\frac{1}{\frac{1}{M}\sum_{i=0}^{M-1}\frac{3}{|P_i|^2}|P_i|^2}} = 3 \qquad \text{(C.7)}$$

and the subchannels of the SC-CP system operating on the boundary.

Case 1: For the SNR region $\Re_{low}, \gamma \le \gamma_0$

$$SNR_{ofdm,i} = \gamma |P_i|^2 \le \gamma_0 |P_i|^2 = \min_i \frac{3}{|P_i|^2}|P_i|^2$$

$$SNR_{ofdm,i} \le 3 \text{ for all i.} \qquad \text{(C.8)}$$

3 is the boundary point of SNR region. And the graph below this boundary is concave. All the subchannels are operating in the concave region of $f(x)$ for any precoder **U.**

Case 2: For the SNR region $\Re_{high}, \gamma \ge \gamma_1$

$$SNR_{ofdm,i} = \gamma |P_i|^2 \ge \gamma_1 |P_i|^2 = \max_i \frac{3}{|P_i|^2}|P_i|^2 = 3$$

$$SNR_{ofdm,i} \ge 3 \qquad \text{(C.9)}$$

The region above the boundary point 3 is convex region. The average BER for this region:

$$BER_{avg} = \frac{1}{M}\sum_{i=0}^{M-1} f\left(\frac{1}{SNR_i}\right) \qquad \text{(C.10)}$$

Using the strictly monotone increasing and convexity properties of the region:

$$\sum_{i=0}^{M-1} \lambda_i f(y_i) \geq f\left(\sum_{i=0}^{M-1} \lambda_i \; y_i\right) \qquad where \;\; \lambda_i \geq 0 \;\; and \qquad \sum_{i=0}^{M-1} \lambda_i = 1$$

Applying this property into the result (C.10) ,

$$BER_{avg} = \frac{1}{M} \sum_{i=0}^{M-1} f\left(\frac{1}{SNR_i}\right) \geq f\left(\frac{1}{M} \sum_{i=0}^{M-1} \frac{1}{SNR_i}\right)$$

$$\frac{1}{M} \sum_{i=0}^{M-1} f\left(\frac{1}{SNR_i}\right) \geq Q\left(\sqrt{SNR_{sc-cp}}\right) = BER_{sc-cp}$$

$$BER_{avg} \geq BER_{sc-cp} \qquad (C.11)$$

$$f\left(\frac{1}{SNR_i}\right) = f\left(\sum_{i=0}^{M-1} |u_{k,i}|^2 \frac{1}{\gamma |P_k|^2}\right) \leq \sum_{k=0}^{M-1} |u_{k,i}|^2 f\left(\frac{1}{\gamma |P_k|^2}\right)$$

$$BER_{avg} = \frac{1}{M} \sum_{i=0}^{M-1} f\left(\frac{1}{SNR_i}\right) = \frac{1}{M} \sum_{i=0}^{M-1} f\left(\sum_{k=0}^{M-1} |u_{k,i}|^2 \frac{1}{\gamma |P_k|^2}\right)$$

$$\leq \frac{1}{M} \sum_{i=0}^{M-1} \sum_{k=0}^{M-1} |u_{k,i}|^2 f\left(\frac{1}{\gamma |P_k|^2}\right) = BER_{avg,ofdm}$$

$$BER_{avg} \leq BER_{avg,ofdm} \qquad (C.12)$$

Using (C.11) and (C.12) for the region $\gamma \geq \gamma_1$,

$$BER_{sc-cp} \leq BER \leq BER_{ofdm} \qquad (C.13)$$

Similarly for the region $\gamma \leq \gamma_0$

$$BER_{ofdm} \leq BER \leq BER_{sc-cp} \tag{C.14}$$

To summarize:

$$For\,the\,concave\,region\,\gamma \in \Re_{low} : \quad BER_{ofdm} \leq BER \leq BER_{sc-cp}$$

$$For\,the\,convex\,region\,\gamma \in \Re_{high} : \quad BER_{ofdm} \geq BER \geq BER_{sc-cp}$$

Convexity analysis for MMSE Receiver

Define a function h as, $h(x) = Q\left(\sqrt{\frac{1}{x} - 1}\right)$. Then the subchannel BER is,

$$Q\left(\sqrt{SINR_i}\right) = h\left(\frac{1}{1 + SINR_i}\right) \tag{C.15}$$

$$\frac{1}{1 + SINR_i} = \sum_{k=0}^{M-1} \frac{|u_{k,i}|^2}{1 + \gamma |P_k|^2} \tag{C.16}$$

$$BER_{avg} = \frac{1}{M} \sum_{i=0}^{M-1} h\left(\sum_{k=0}^{M-1} \frac{|u_{k,i}|^2}{1 + \gamma |P_k|^2}\right) \tag{C.17}$$

The function $h(x) = Q\left(\sqrt{\frac{1}{x} - 1}\right)$ is convex because $h'(x) > 0$ and $h''(x) \geq 0$. From the convexity and strictly monotone increasing property of $h(x)$,

$$\frac{1}{M} \sum_{i=0}^{M-1} h\left(\frac{1}{1 + \gamma |P_i|^2}\right) \geq h\left(\frac{1}{M} \sum_{i=0}^{M-1} \frac{1}{1 + \gamma |P_i|^2}\right) \tag{C.18}$$

i.e.

$$BER_{avg,OFDM} \geq BER_{avg,\,SCCP} \tag{C.19}$$